



An algorithm for detecting *Trichodesmium* surface blooms in the South Western Tropical Pacific

Cecile Dupouy, D. Benielli-Gary, Jacques Neveux, Yves Dandonneau, T. K. Westberry

► To cite this version:

Cecile Dupouy, D. Benielli-Gary, Jacques Neveux, Yves Dandonneau, T. K. Westberry. An algorithm for detecting *Trichodesmium* surface blooms in the South Western Tropical Pacific. *Biogeosciences*, 2011, 8, pp.3631-3647. 10.5194/bg-8-3631-2011 . hal-00875926

HAL Id: hal-00875926

<https://hal.science/hal-00875926>

Submitted on 23 Oct 2013

HAL is a multi-disciplinary open access archive for the deposit and dissemination of scientific research documents, whether they are published or not. The documents may come from teaching and research institutions in France or abroad, or from public or private research centers.

L'archive ouverte pluridisciplinaire **HAL**, est destinée au dépôt et à la diffusion de documents scientifiques de niveau recherche, publiés ou non, émanant des établissements d'enseignement et de recherche français ou étrangers, des laboratoires publics ou privés.

An algorithm for detecting *Trichodesmium* surface blooms in the South Western Tropical Pacific

C. Dupouy¹, D. Benielli-Gary², J. Neveux³, Y. Dandonneau⁴, T. K. Westberry⁵

[1] LOPB - Laboratoire d'Océanographie Physique et Biogéochimique, UMR 6535, CNRS-INSU-IRD-Université de la Méditerranée, 1M213, Centre de Nouméa, B. P. A5, New Caledonia

[2] LAM - Laboratoire d'Astrophysique de Marseille, Pôle de l'Étoile Site de Château-Gombert 38, rue Frédéric Joliot-Curie 13388, Marseille Cedex 13, France

[3] CNRS, UMR7621, Observatoire Océanologique de Banyuls, Laboratoire d'Océanographie Microbienne, Avenue Fontaulé, F-66651 Banyuls sur Mer, France

[4] Université de Paris VI-UPMC-LOCEAN and 14 rue de la Victoire, 91740 Chamarande, France

[5] Dep. Botany Plant Pathology, Oregon State University Corvallis, USA OR 97331-2902

*Cecile.dupouy@ird.fr, tel: 687 26 43 26, fax: 687 26 07 29

Running title: *Trichodesmium* surface blooms in the SW Pacific

Abstract

Trichodesmium, a major colonial cyanobacterial nitrogen fixer, forms large blooms in NO₃-depleted tropical oceans and enhances CO₂ sequestration by the ocean due to its ability to fix dissolved dinitrogen. Thus, its importance in C and N cycles requires better estimates of its distribution at basin to global scales. However, existing algorithms to detect them from satellite have not yet been successful in the South Western Tropical Pacific (SP). Here, a novel algorithm (TRICHODESMIUM SATellite) based on radiance anomaly spectra (RAS) observed in SeaWiFS imagery, is used to detect *Trichodesmium* during the austral summertime in the SP (5°S-25°S 160°E-170°W). Selected pixels are characterized by a restricted range of parameters quantifying RAS spectra (e.g. slope, intercept, curvature). The fraction of valid (non-cloudy) pixels identified as *Trichodesmium* surface blooms in the region is low (between 0.01 and 0.2 %), but is about 100 times higher than deduced from previous algorithms. At daily scale and in the SP, this fraction represents a total surface oceanic area varying from 16 to 48 km² in Winter and from 200 to 1000 km² in Summer (and at monthly scale, from 500 to 1000 km² in Winter and from 3100 to 10890 km² in Summer with a maximum of 26432 km² in January 1999. The daily distribution of *Trichodesmium* surface accumulations in the SP detected by TRICHOSAT is presented for the period 1998-2010 which demonstrates that the number of selected pixels peaks in November-February each year, consistent with field observations. This approach was validated with in situ observations of *Trichodesmium* surface accumulations in the Melanesian archipelago around New Caledonia, Vanuatu and Fiji Islands for the same period.

Keywords: *Trichodesmium*, surface blooms, radiance anomaly spectra, algorithm, SeaWiFS, ocean color, New Caledonia, Vanuatu, Fiji Islands, Tropical Pacific Ocean, Melanesian archipelago.

1. INTRODUCTION

The balance between oceanic N₂ fixation and nitrogen losses (denitrification) in the ocean has been postulated to regulate atmospheric CO₂ over geological time via the enhancement of biological sequestration of CO₂ (Falkowski, 1997; Gruber and Sarmiento, 1997; Deutsch et al., 2007; Capone and Knapp, 2007). Unicellular (Zehr et al., 2001; Montoya et al., 2004; Church et al., 2008; 2009; Zehr et al., 2011) and filamentous cyanobacteria (Carpenter, 1983; Capone et al., 1997; Capone et al., 2005; LaRoche and Breitbarth, 2005; Bonnet et al., 2009; Moisander et al., 2010) incorporate this form of “new” nitrogen (N) into the marine food web of tropical and subtropical oceans (Berman-Frank et al., 2004; Mahaffey et al., 2005; Mulholland, 2007). N₂ fixation is considered to be the major source of new N in stratified, oligotrophic tropical oceans (Capone et al., 1997; Karl et al., 2002). Future change in sea surface temperature (Breitbarth et al., 2006) or/and CO₂ concentration are expected to stimulate photosynthesis (C fixation) and N₂ fixation by filamentous cyanobacteria, particularly by *Trichodesmium* spp. (Barcelos et al., 2007; Hutchins et al., 2007; Kranz et al., 2009; Levitan et al., 2010). This enhancement of *Trichodesmium* growth could compensate the decreased growth of other phytoplankton owing to a presumed decrease of nitrate supply.

Trichodesmium spp. can form extensive blooms which have been observed for a long time in the South Western Pacific Ocean (SP), particularly in austral summer (Dandonneau and Gohin, 1984). The presence of three major archipelagos (New Caledonia, Vanuatu and Fiji-Tonga in the SP region ([5°S- 25°S, 150°E- 170°W], Figure 1a) and their potential for oceanic iron enrichment from land may trigger these cyanobacterial blooms (Bowman and Lancaster, 1965; Mantas et al., 2011) as *Trichodesmium* blooms require large quantities of iron (Rubin et al., 2011). The blooms appear as brown or orange meandering patterns around those archipelagos (Dupouy et al., 1988; Dupouy, 1990; Tenório, 2006; Hashihama et al., 2010), are clearly detected from the International Space Shuttle (December 2001 around Tonga Islands), and were recently highlighted by the NASA Ocean Color Website (Feldman et al., 2010). Blooms are also regularly observed in waters of the Dampier Archipelago, the Arafura Sea (Neveux et al., 2006) and off the Great Barrier Reef (Kuchler and Jupp, 1988; Furnas, 1989; Bell et al., 1999). *Trichodesmium* was reported in the Western North Pacific (Shiozaki et al., 2009; Kitajima et al., 2009; Konno et al., 2010). Nevertheless, observations in the SP contradict the recently published global map of *Trichodesmium* analogs based on ecosystem

1 model results that indicate a predominance of higher densities in the North Pacific than in the
2 South Western Pacific Ocean (Monteiro et al., 2010).

3 Estimating the occurrence of *Trichodesmium* surface blooms from satellite is a major
4 challenge, but will be required for large-scale estimates of nitrogen fixation (e.g., Westberry et
5 al., 2005; Westberry and Siegel, 2006). Regional algorithms have been successfully applied
6 on the Atlantic continental shelf (Subramaniam et al., 2002), off Canary Islands (Ramos et al.,
7 2005) as well as the Indian coast (Sarangi et al., 2004). Global algorithms have also been
8 recently developed for estimating phytoplankton community structure in the surface oceans.
9 PHYtoplankton SATellite (PHYSAT) algorithm was successful in identifying *Synechococcus*-
10 like cyanobacteria with maxima in the tropics, and found that they are particularly abundant in
11 the tropical ocean (Alvain et al., 2005). The Scanning Imaging Absorption Spectrometer for
12 Atmospheric Cartography (SCHIAMACHY) sensor also detects a cyanobacterial signal
13 within the same latitudinal band (Bracher et al., 2008). However, all algorithms generally fail
14 at identifying seasonality of *Trichodesmium* blooms in the SP and none retrieve the relatively
15 high abundance of *Trichodesmium* surface blooms expected and observed in situ during
16 austral summer (November to March). Here we develop an algorithm to detect
17 *Trichodesmium* surface blooms in the SP which is based on SeaWiFS radiance anomalies
18 (similar to PHYSAT) and apply it to SeaWiFS data from 1997-2010.

20 2. MATERIAL AND METHODS

21 2.1. DATA

22 2.1.1. In situ observations

23 Bloom observations (Figure 2) included these done during the maritime survey of the
24 Economic Exclusive Zone of New Caledonia by the French Navy (aerial and shipboard
25 observations) and these obtained during scientific cruises on the R/V *Alis* between New
26 Caledonia, Vanuatu, Fiji and Wallis and Futuna Islands (15°S to 23°S, 160°E to 180°E;
27 Dupouy et al., 2004a). At most of the observation by the French Navy and the R/V *Alis*,
28 surface water samples was collected with bucket and preserved on board in a 4% formalin
29 solution. Then, identification of diazotroph morphological groups was made under a Zeiss
30 microscope at IRD Nouméa (LOCEAN laboratory). Furthermore, between October 2001 and
31 October 2003 (nine Diapalis cruises as part of the DIAzotrophy in a Pacific ZONE program),
32 more detailed identification and abundance distribution of filamentous diazotrophs was

obtained from inverted microscopy (Tenório, 2006). In this case, sampling was done with 8 L Niskin bottles (sometimes with bucket sampling for comparison). During the Diapalis cruises, chlorophyll and phycoerythrin measurements were obtained from spectrofluorometry (Lantoiné and Neveux, 1997; Neveux et al., 1999; Neveux et al., 2006). A slightly higher concentration of chlorophyll a (Chl *a*) was observed from bucket samples compared to those from Niskin samples.

2.1.2 Satellite ocean color data

For the development of the new algorithm, representative global SeaWiFS Level3 data (R2009) were selected at summer and winter seasons, and included normalized water leaving radiance, $nLw(\lambda)$, at 6 channels (412, 443, 490, 510, 555, and 670 nm) as well as SeaWiFS chlorophyll and the diffuse attenuation coefficient at 490 nm (K490 product). From these data, a Look Up Table (LUT) relating K490 to remote sensing reflectance was created (see Section 2.2). However, to avoid compositing artifacts upon application of the LUT, daily SeaWiFS Level-2 GAC (R2009) between 1998-2010 and covering the Western Pacific Ocean (160°E-160°W/25°N-25°S area), were used.

2-2. METHODS

The general approach was to define a spectral radiance anomaly from SeaWiFS $nLw(\lambda)$ that was specifically related to *Trichodesmium* surface blooms. It aimed at removing the first order variability in ocean color caused by chlorophyll concentration while preserving the variability that may be specifically caused by individual phytoplankton species or other optically active components. This objective is similar to the PHYSAT classification method (Alvain et al., 2005) that was initially developed for discrimination of major phytoplankton groups in Case 1 waters. Waters dominated by diatoms, *Prochlorococcus*, *Synechococcus*-like cyanobacteria or haptophytes could thus be classified according to their radiance anomaly spectra (RAS):

$$nL^*w(\lambda) = nLw(\lambda) / \langle nLw(\lambda) \rangle \quad (1)$$

where $\langle nLw(\lambda) \rangle$ is the expectation of nLw at a given chlorophyll concentration, computed as the average of a large global SeaWiFS dataset, and nL^*w is the radiance anomaly relative to this average. The main advantage of PHYSAT is to provide thresholds allowing

1 characterization of RAS at each pixel. PHYSAT uses LUT of $\langle nLw(\lambda) \rangle$ as a function of
2 chlorophyll.

3 Here, we employed a LUT based on the diffuse attenuation coefficient at 490 nm
4 (SeaWiFS “K490”). K490 has the advantage over chlorophyll of being computed
5 straightforwardly while operational SeaWiFS chlorophyll estimates result from switching
6 between three wavelength ratios. This new LUT was built using four daily, global Level-3
7 images from February 15, May 15, August 15 and November 15 2002, in order to encompass
8 a seasonal cycle. The LUT contains the likelihood of SeaWiFS radiances, noted $\langle nLw(\lambda)_{K490} \rangle$
9 \rangle , for all K490 values in the 0.0186 m^{-1} to 0.2499 m^{-1} interval. Radiance anomaly spectra
10 (RAS) are then computed as

$$11 \quad nL*w_{K490}(\lambda) = nLw(\lambda) / \langle nLw(\lambda)_{K490} \rangle \quad (2)$$

12 where $nLw(\lambda)$ are the SeaWiFS radiance estimates. At the end, we checked that results are
13 strictly equivalent than when Chlor_a is used as in PHYSAT. Radiance anomaly spectra
14 $nL*w_{K490}$, hereafter denoted RAS, can thus be considered as equivalent than PHYSAT
15 nLw^* .

16 There is another significant difference between the approach used here compared with the
17 previous PHYSAT effort. Instead of defining RAS thresholds and associating them with
18 pigment classes (and thus, different phytoplankton groups), the new algorithm defines
19 quantitative shape and magnitude criteria of the RAS itself. Eighteen summer scenes around
20 New Caledonia in 2003 and 2004 were selected as they correspond to periods where slicks
21 and high abundance ($> 5000 \text{ trichomes.L}^{-1}$) of *Trichodesmium* was observed in the surface
22 ocean (Tables 1 and 2). In 2003, SeaWiFS level2-GAC of January 6, 13, 18, February 1, 4, 9,
23 13, 16, 18, 21, 28, March 2, 6; Yeardays: 6, 13, 18, 32, 35, 40, 44, 47, 49, 52, 59, 62, 66)
24 corresponded to slicks observations by the French Navy from December 2002 to February and
25 March 2003 (Table 1). The gap between December 2002 and February 2003 may be due to
26 the January 2003 cyclone “Beni” that prevented sea observations. In 2004, SeaWiFS level 2-
27 GAC of February 10, 18, 23, and March 3, 17; Yeardays 41, 48, 53, 63, 77), corresponded to
28 slicks observations from January to March 2004 (Table 1). The definition of the RAS of
29 *Trichodesmium* surface blooms on the SeaWiFS satellite imagery was generated for pixels
30 around New Caledonia and Fiji from these 18 scenes.

31 The criteria have been chosen in such a way that they permit to rebuild RAS spectra. The
32 RAS was calculated and the “shape” and magnitude criteria of this RAS examined. RAS

spectra could be described by the coefficients of a polynomial fit (degree 2) (Figure 3a). We thus retained the following criteria for an objective description of the *Trichodesmium* RAS 1) slope of the linear fit of RAS vs wavelength (S), and 2) the ordinate of the polynomial fit for which the tangent is parallel to linear fit (Yt). Additional criteria related to the shape of the RAS were defined as the major positive and major negative deviations relative to the second degree polynomial fit (largest “bump” or largest “trough”, respectively).

3. RESULTS

3.1 FIELD OBSERVATIONS

Aerial and shipboard visual observations of *Trichodesmium* surface blooms (Figure 1b, c) around New Caledonia between 1998 and 2004 are presented in Table 1 and average cruise and transect surface biomass and abundance are presented in Table 2.

Generally, slick sizes were a few tens of meters wide and two to three nautical miles long (shipboard or aircrafts photographs, Figure 2). Twice in the series (November 1998, November 1999) large areas of 30 km² were covered by slicks, and once in February 2004, the whole area between New Caledonia and Vanuatu (300 km²) was covered by numerous elongated slicks well detected by longline aircrafts. *Trichodesmium* was responsible of the majority of the slicks observations. Only one formalined sample (12 December 2002) contained small pumices originated from Vanuatu or Tonga volcanoes which were mixed with the *Trichodesmium* colonies. Sea-rafterd pumices can drift to the west and reach New Caledonia. Some of these rafts reached the Australian coast in October 2002, approximately 7-8 months after a submarine eruption in the Tonga Trench (Bryan et al., 2004). None of the slick observations corresponded to coral spawning which is responsible of fugitive coastal red waters once a year in New Caledonia. The abundance of *Trichodesmium* spp. in the SP exhibited a strong seasonality as previously pointed out (Dupouy et al., 2004a; Moutin et al., 2005) with the highest number of visual observations (65% or 61 over 93 total observations) over the study period (November 1998 to June 2010) occurring between December and February (Table 1). Surface blooms were never detected during winter (only one observation of slicks was available in July 2002, at the west of Fiji Islands, Table 1). Nearly every year, surface blooms developed between New Caledonia and Vanuatu and one of these blooms was exceptionally well tracked (February 2004, Table 1). Slicks were first observed in November 2003 near Vanuatu (17.65°S, 167.56°E), in December 2003 at the north and south of New

Caledonia, in January (on 26 at 22°S and on 29-30 at 20.33°S/ 166.12°E) then in February 2004 (on 1st around New Caledonia and on 12-16 near Vanuatu and again North of New Caledonia at 19.49.9°S, 169. 54°E). The surface bloom persisted after heavy rains and wind-mixing by Category 4 cyclone Ivy on February 24. It was detected near New Caledonia (on February, 26), and under calm meteorological and sea conditions, its slick was sampled on February 28 showing an orange surface scum (around 21°S, New Caledonia) or large flocks of dead colonies (at 18.55°S, 166.05°E, Vanuatu) which disappeared in the evening (17.38°S, 166.07°E) (Motevas cruise, Table 2). In March, white senescent *T. erythraeum* (March 1-4, at 22°S, 167°E and 20.16°S/168.71°E) and remnant coastal slicks on (March 29) were seen near Vanuatu (17°S, 167°E). In April, remnant slicks were seen nearby Lifou island at the east of the "Grande terre" of New Caledonia (Table 1). Surface slicks were also observed in summer during a water-column observational program in the Loyalty Channel (12 October 2001, 5 February 2003 and 2004, see Table 1 and Table 2).

Among the pelagic species described in the Pacific region (Revelante and Gilmartin, 1982; Carpenter et al., 1993), a high morphological diversity of filamentous cyanobacteria as described by Lundgren et al. (2005) and Tenório (2006) was observed in our surface samples (Figure 1c). Colonies were essentially composed of small rafts from 10 to 50 filaments, small in length (noted *T. erythraeum*), or long and twisted rafts (noted *T. thiebautii*) of 50-100 filaments. Long and curved filaments composed of cells larger than long, and some thinner filaments with cells 5-6 fold longer than wide were noted *K. pelagica* and *T. tenue*, respectively. The distribution of these four morphotypes is shown in Figure 1c. There is no evidence that the same *Trichodesmium* genus or species is widespread all over the tropics except for the *Katagnymene* form (Lundgren et al., 2005). We tended to find *T. erythraeum* near the New Caledonia mainland but elsewhere most of the morphotypes were mixed. During the peak observed *Trichodesmium* abundance in 2004, and along a transect from New Caledonia (20-21°S) to Vanuatu (19°S -17°S), short tufts of *T. erythraeum* were observed at the beginning of the transect (NC) and a mix of *T. thiebautii* (50%), *T. tenue* (25%), *erythraeum* (15%), and *Katagnymene pelagica* and *spiralis* (10%) dominated populations at the end (Vanuatu). This population change was also seen in fluorescence excitation spectra of phycoerythrin (change in the phycourobilin/phycoerythrobilin ratio, as in Neveux et al., 2006). Mixed assemblages of *T. erythraeum*, *T. thiebautii*, and *T. contortum* filaments were also observed on the 2nd and 9th of February 2005 around Fiji Islands (Hashihama et al., 2010), while floating puffs and tufts of mixed taxonomy were observed in March 2007

(Biegala, pers. com.). Only *K. pelagica* + *T. tenue* colonies were found isolated near the Niue Island at 19° 2' S 169° 52' W (Table 1, Figure 1c).

Surface *Trichodesmium* abundance and associated biomass (Chl *a* > 10 µm) in the Loyalty Channel and along transects between New Caledonia, Vanuatu or Wallis and Futuna allowed to determine a seasonal variability (Table 2). Low filament densities characterized the end of the bloom season in April 1998 and *Trichodesmium* contribution to biomass was reduced (Dupouy *et al.*, 2000; Campbell *et al.*, 2006), as in April 2002 and 2003 (Table 2). High abundance was never observed in May, except in 2002 along the transect 1, where phycoerythrin spectral characteristics confirmed the dominance of *Trichodesmium* between New Caledonia and Vanuatu. At the beginning of the summer season (October), densities were high in 2001 but null in 2003. *Trichodesmium* abundance was always higher in summer, except during two 2001-2002 Diapalis cruises (December, January). During Motevas in February 2004 (Dupouy *et al.*, 2004b; Dupouy *et al.*, 2008), the beam attenuation was high (0.1 m⁻¹), and a maximal *Trichodesmium* contribution to Chl *a* of 50-70% was observed with a high density of 5000 filaments.L⁻¹ and maximal biomass of 1.9 and 14 mg.m⁻³ for Chl *a* and phycoerythrin, respectively. Densities were similar to those measured during February 2003 during Diapalis 07 (Tenório, 2006; Neveux *et al.*, 2006; Masotti *et al.*, 2007). The determination of biomass in surface slicks was difficult and will need a specific thin-layer surface sampler. Nevertheless, Chl *a* concentrations up to 2 µg L⁻¹ in the ocean and 3 mg L⁻¹ in the New Caledonia lagoon were observed (Tenório, 2006). In winter, *Trichodesmium* abundance was always low and relatively high chlorophyll values were associated with small size algae (low values of the Chl *a* fraction above 10 µm).

3.2 DETECTION OF TRICHODESMIUM IN SATELLITE DATA

In summer 2003 and 2004, the majority of pixels for the region around New Caledonia exhibited the same RAS. These RAS characteristics were examined under the assumption that instances where Chl *a* > 0.2 mg.m⁻³ were dominated by *Trichodesmium* while those with < 0.2 mg.m⁻³ were not, similar to in situ observations. For Chl *a* > 0.2 mg.m⁻³, linear slopes of the RAS varied between -0.005 and 0.008, and the tangent ordinate Yt varied within a range of 0.8 to 1.4. For Chl *a* < 0.2 mg.m⁻³, the RAS slope varied within -0.005 to 0.012, while Yt also varied between 0.8 to 1.4. A narrow range of slopes S (S between -0.0019 and -0.0017) and intercepts Yt (Yt from 0.9725 to 1.0175) characterized *Trichodesmium* pixels (Figure 1b). These ranges corresponded to low but not minimal values of the total slope range [-0.005 to +

0.012], and to a narrow interval of values of the total intercept Y_t range [0.8 to 1.4]) (Figure 3b). Moreover, it was found that RAS of pixels corresponding to *Trichodesmium* surface blooms had a specific shape. These RAS spectra were characterized by: 1) lack of a “bump” at 555 nm (flat RAS or trough at 555 nm) and 2) always a “bump” at 670 nm and never a trough at 670 nm (Figure 3b). Criteria for 412, 443, 490 and 510 nm were rather neutral. No weighting of these criteria was necessary for the selection of pixels which approach this ideal shape. The criteria of the RAS for the 555 nm and 670 nm SeaWiFS channels were essential while the criteria for other wavelengths were less useful. On the contrary, quantitative criteria of the RAS defined as in Figure 3b were discriminant. Ultimately, it appeared that the special RAS shape and quantitative criteria was independent of the Chl_a of the pixels.

The application of *Trichodesmium* RAS criteria (TRICHODESMIUM by SATellite algorithm: TRICHOSAT) to all SeaWiFS Level-2 data from 1997 to 2010 within the whole Western Pacific ocean region [25°N- 25°S and 160°E -160°W, noted WP] is shown as composites in Figure 4 for the interseason (April-May, October). The application of the shape criteria and the quantitative criteria separately were not sufficient to discriminate *Trichodesmium* surface bloom pixels (Figure 4b and 4c). The TRICHOSAT algorithm finally selected the pixels which satisfy both criteria (Figure 4d), i.e. the intersection of the two groups selected by the shape criteria or the quantitative criteria. The resulting composite Figure 4d shows that the majority of selected *Trichodesmium* pixels is in the SP. Note that the algorithm selection differs markedly from the distribution of pixels with Chl_a concentration greater than 0.2 mg.m⁻³ (Figure 4a) as there are no *Trichodesmium* pixels in the huge equatorial upwelling maximum, and only few pixels in the northern part of the Pacific Ocean. *Trichodesmium* flagged pixels are not necessarily associated with high chlorophyll content pixels, similar to [Westberry and Siegel \(2006\)](#).

In order to get statistically coherent results for the comparison of the percentage of *Trichodesmium* pixels identified for each year and season, it was verified that a sufficient number of processed SeaWiFS Level-2 GAC images (5×10^4 - 1×10^6 pixels with quasi equivalent numbers of non-cloudy valid pixels for each season) were analyzed (Figure 5).

Trichodesmium bloom distributions by TRICHOSAT for the WP are shown as composites over 12 years for each of the three seasons (winter, interseason, and summer) on Figure 6abc. The increase in selected *Trichodesmium* pixels from austral winter (Figure 6a) to the interseason (Figure 6b) to austral summer (Figure 6c) in the SP is visually evident. Although there is a relatively high response of TRICHOSAT between 1998 and 1999 during boreal winter in the northern Pacific (November-December 1998 (in yellow); January-March

1999 (in black)) around 160°W, no *Tricho* pixels were retrieved in the 2000-2010 years at that season.

Figure 7a shows the temporal evolution of the percentage of *Trichodesmium* bloom pixels identified by TRICHOSAT on a monthly basis. The algorithm was applied to the WP and to the SP boxes. Regular peaks were observed from Dec-Feb nearly every year over the 12-year period examined, albeit with strong inter-annual variations in the monthly maximum percentage of retrieved *Trichodesmium* pixels exhibited strong inter-annual variations. For the SP box, the percentage was above 0.2 % in 1999 and in 2004-2005 and dropped to 0.01% in winter. At monthly scale, this fraction represents a total number of *Trichodesmium* bloom pixels varying from 31 to 62 in Winter and from 193 to 680 in summer compared to a number of valid (non-cloudy) pixels varying between 200×10^3 and 10^6 pixels with a maximum of 1652 in January 1999. This is equivalent to monthly surface areas varying between 500 to 1000 km² in Winter and from 3100 to 10890 km² in Summer with a maximum of 26432 km² in January 1999. For the WP box, the percentage was much reduced with a maximum of 0.03%. Indeed, the percentage was comparatively greater for SP box because there were much less *Trichodesmium* pixels detected in the northern half of the domain. The mean monthly chlorophyll concentration extracted from Giovanni for the SP is also shown. Note that only a few *Trichodesmium* peaks correspond to a secondary chlorophyll maximum, which further illustrates the independence of bloom occurrence and chlorophyll concentration.

The mean seasonal cycle of the *Trichodesmium* bloom pixels monthly percentage detected for the 1997-2010 period in the SP is shown at Figure 8ab. Over 12 years, *Trichodesmium* bloom pixels maximum were observed in January and February with relatively high inter-annual variation. Similarly, the 12-y average monthly percentage of slick observations (from Table 1, and [Moutin et al., 2005](#) for observations before 2004), peaks between January and February.

TRICHOSAT was also applied to single daily level 2-GAC images around New Caledonia and Vanuatu and for short periods representative of summer and winter months (Figure 9ab). From the 10th to the 22th of February 2003, TRICHOSAT selected pixels spread out between Vanuatu and the northwestern part of New Caledonia and Fiji (Figure 9a). Two observations from the French Navy coincide with TRICHOSAT pixels. From the 9th to the 15th of June 2003, no pixels were detected around New Caledonia (Figure 9b). The few *Trichodesmium* pixels at the southern limit of the equatorial upwelling between 7°S and 5°S could correspond to observations of *Trichodesmium* blooms in the southern and northern convergence zones of the upwelling ([Lebouteiller et al., 1992](#); [Blanchot, pers.com.](#)).

The comparison between in situ observations of slicks (summed by month from Table 1) and the percentage of *Trichodesmium* bloom pixels detected on each single level-2 GAC by TRICHOSAT in the SP for the total 1998-2010 period is shown at Figure 10. The striking coincidence between the number of observations of surface slicks (from 1 to 6 between October 2003 and February 2004) and the peak of percentage of pixels screened by TRICHOSAT is the result of favorable observation conditions in the SP. Despite the reduced amount of observations out of the 2003-2004 period, the maximum percentage of *Trichodesmium* bloom pixels generally corresponds to a significant number (> 2) of observed slicks (Figure 10).

4. DISCUSSION

4.1- GENERAL CONSIDERATIONS OF THE ALGORITHM

A rather linear RAS spectrum

TRICHOSAT identifies pixels for which the RAS is characterized by a narrow range of S (small negative numbers) and of Yt (values near 1) which implies a relatively linear RAS spectrum compared with the total range of S and Yt found within the whole Pacific Ocean. Shape criteria (bumps and troughs), of the RAS are also essential as the intersection between shape and RAS quantitative criteria is required for the successful selection of *Trichodesmium* bloom pixels (Figure 4bcd). This means that the RAS spectra of *Trichodesmium* blooms are very similar to what is expected at a given chlorophyll concentration contrary to other phytoplankton groups for which the PHYSAT approach is based specifically on low or high reflectance relatively to the detected chlorophyll content (Alvain et al., 2005). Westberry et al. (2005) also found remarkably similar bulk reflectance spectra for cases which contained moderate amounts of *Trichodesmium* compared to those where it was absent.

A rather weak relationship with biomass

The RAS is by definition, independent of chlorophyll concentration (second order anomaly). Therefore, it is not surprising that selected pixels correspond to a large range of Chl_a values, from 0.07 to 0.3 mg.m⁻³ in single level2-GAC images. It has already been shown that chlorophyll associated with surface accumulations of *Trichodesmium* is highly variable. Also, a well-known underestimation of chlorophyll by SeaWiFS due to a strong package effect in filaments and colonies (Subramaniam et al., 1999; Dupouy et al., 2008) was observed but this

would concern only living colonies. As TRICHOSAT probably screens pixels containing high *Trichodesmium* concentrations mixed in the upper oceanic layer or forming surface accumulations, this might alter the relationship between reflectance and chlorophyll concentration.

Comparison with previous algorithms

The percentage of TRICHOSAT selected pixels in the New Caledonia region (Figure 7, 8, 10) is low (maximum 0.2% of total valid pixels). TRICHOSAT was set to detect a specific case of *Trichodesmium* bloom. This configuration is when *Trichodesmium* is concentrated on 1 mm or maybe more, and visible by eye. Densities are then between 17000 trichomes.L⁻¹ to 39 10⁶ trichomes.L⁻¹ (Devassy et al., 1978). Assuming a strong accumulation which contains about 3 mg.L⁻¹ Chl *a* distributed on a 1 mm thickness, this is equivalent to an integrated concentration of 3 mg.m⁻² of Chl *a* related to *Trichodesmium*. If the bloom occupies an area of 100 m², i.e. the 1/160000e of the pixel size, the mean Chl *a* concentration linked to *Trichodesmium* in the pixel is 0.018 mg m⁻². Supposing that the rest of the phytoplankton represents on average 0.1 mg.m⁻³, we need about 500 m² of concentrated accumulation within the pixel to double the chlorophyll concentration. The probability of finding *Trichodesmium* bloom pixels is low as the probability to observe a 500 m² concentrated patch within a pixel, is also weak. Nevertheless, the algorithms of [Subramaniam et al. \(2002\)](#) and [Westberry et al. \(2005\)](#) (hereafter denoted as W05) detect even fewer pixels (100 times less). In the SP, the W05 algorithm retrieves only highly reflectant pixels, most of which correspond to the extremely high reflectance of New Caledonia or Fijian sandy lagoons or Islands. Furthermore, apart from the coastal lagoon pixels, only 15 points are identified as *Trichodesmium* by W05 and there is no indication of seasonal variation. Recall that the W05 algorithm was built to detect *Trichodesmium* at bloom concentrations (Chl *a* threshold for a bloom was set to 0.8 mg.m⁻³) while TRICHOSAT detection does not imply Chl *a* concentration threshold. The rather weak spectral anomalies of *Trichodesmium* pixels may explain why W05 does not detect more blooms in the SP. The first published set of criteria for screening pixels containing *Trichodesmium* overemphasized backscattering (for $\lambda > 500$ nm) and Colored Dissolved Organic Matter (CDOM) absorption (for $\lambda < 440$ nm) so that finally a refined model using subtle variations in reflectances between phytoplankton and *Trichodesmium* spectra had to be used ([Westberry and Siegel, 2006](#)). In the SP, *Trichodesmium* bloom signatures may not be

strong enough to be detected by W05, or blooms occur in filaments whose signatures may not be strong enough to affect 16 km² pixels. Finally, living colonies of *Trichodesmium* are often associated with other phytoplankton as observed during the Diapalis 7 cruise (Tenório, 2006) and serve to create a mixed optical signal obfuscating detection. *Trichodesmium* biomass could then be well below the W05 detection threshold, and/or the other phytoplankton biomass would be higher in proportion in the SP than in the northern hemisphere. This may also explain why the W05 algorithm detects similar *Trichodesmium* pixel numbers in winter and in summer. Overall, TRICHOSAT was tuned to detect the *Trichodesmium* blooms that we have observed in the field in summer, and the W05 algorithm fails to detect these blooms.

4.2 OPTICAL VALIDATION OF THE ALGORITHM

Ideally, one would validate the RAS of TRICHOSAT detected *Trichodesmium* pixels with *in situ* radiometric measurements made in *Trichodesmium* surface blooms. Unfortunately, such a task is difficult as there is no direct measurement of the RAS which would require accurate measurements of above/in water reflectance. Past work has recognized this as problematic (Subramaniam et al., 1999; Kutzer, 2009). Recall that the *Trichodesmium* bloom RAS is defined by a very small range of S and Yt. This implies that SeaWiFS spectra are not so different from what they are expected at a given K₄₉₀ (i.e. at a given Chl_a) despite the fact that filamentous cyanobacteria blooms appear brighter than surrounding water areas due to high backscattering associated with gas vesicle and to a microbiotope (bacteria, detritus) (Subramaniam et al., 1999).

One of the TRICHOSAT shape criterion is that the RAS must never show a bump at 555 nm. It is well known that reflectance spectra of colonies, assembled on filters (Dupouy et al., 2008) are characterized by a succession of troughs, each trough corresponding to different pigment absorption maxima (e.g., chlorophyll, phycourobilin and phycoerythrobilin). Phycoerythrin absorption in green wavelengths are observed in *Trichodesmium* suspension (PSICAM measurements, Dupouy and Röttgers, 2010), in raw H6-backscattering spectra (absorption at 550 nm along the pathway of backscattered light (Dupouy et al., 2008), and observed *in situ* during the 2004 bloom (unp. data)).

The second robust criterion is that the RAS must never show a trough at 670 nm (rather a bump at 670 nm). It has been shown that high near-infrared reflectance is observed if colonies are accumulated on top of the water (Subramaniam et al., 1999; Dupouy et al., 2008). RAS would then depend on the proportion of colonies lying above the water surface which will

1 depends on thickness, or/and on the physiological characteristics of colonies, or age of the
2 bloom (Dupouy et al., 1990; 1992; Dupouy et al., 2008). The high reflectance of blooms at
3 670 nm which was observed with the Coastal Zone Colour Scanner (CZCS) could provide an
4 approach to detecting slicks for MODIS (Hu et al., 2010; McKinna et al., 2011) or IRS-P4
5 OCM (Sarangi et al., 2004).

6 There was no robust criteria for the RAS at 412 nm even though a significant RAS feature
7 was expected at this wavelength as it has been shown that Dissolved Organic Carbon (DOC)
8 and CDOM is released from dead or living colonies (Subramaniam et al., 1999). Optical
9 characteristics of surrounding waters may also be important for defining RAS of
10 *Trichodesmium* blooms. As seen in Figure 7b, the dissolved matter + detritus absorption
11 coefficient, ACDM (derived from the GSM optical inversion model at 412 nm; Maritorena et
12 al., 2002), for the SP box experiences a strong seasonal variation due to the well documented
13 annual cycle of solar bleaching and photolysis in the South Pacific (Siegel et al., 2002; 2005).
14 *Trichodesmium* surface blooms correspond to the period of minimum CDOM concentration in
15 summer. In the SP, some peaks are associated with a secondary CDOM maximum which
16 could be produced by blooms (e.g., February 1999, 2003, 2004 and 2006). In contrast, the
17 particulate backscattering coefficient, b_{bp} (also derived from Maritorena et al. (2002) was
18 rather constant though noisy over the 12-year period (Figure 7b). *Trichodesmium* blooms
19 correspond to the period of minimum backscattering, as a weak maximum appears in June-
20 September (more or less in phase with chlorophyll concentration). The b_{bp} cycle in the SP
21 could be linked to small-sized detritus as suggested by Loisel et al. (2006) rather than to
22 *Trichodesmium* blooms.

23 The relatively high response by TRICHOSAT in the northern Pacific around 160°W
24 between 1998 and 1999 during boreal winter (November-December 1998 (in yellow);
25 January-March 1999 (in black)) do not correspond to visual observations of blooms in this
26 area (Dore et al., 2008). From 2000 to 2010, no *Trichodesmium* pixels were retrieved during
27 boreal winter in the Northern Pacific area by TRICHOSAT. We have no explanation for what
28 happened during the 98-99 boreal winter period near Hawaii. We conclude that there is some
29 signal there picked up by the TRICHOSAT algorithm. Blooms of unknown origin were
30 already reported using CZCS observations in December (Dore et al., 2008). This has to be
31 caused by floating living material similar in reflectance to *Trichodesmium* and therefore
32 having the same SeaWiFS RAS. Also, there may be a different relation between reflectance
33 and K_{490} in SeaWiFS data for these five months than for the rest of the studied period. A new

research on this zone should be done to determine the nature of this optical signal in the Northern Pacific.

4.3 RELATIONSHIPS WITH OTHER CYANOBACTERIA IN THE WATER COLUMN

The austral summer maxima of surface blooms detected with TRICHOSAT in SP (Figure 7a) corresponds with the inter-annual variations of *Trichodesmium* abundances in the surface layer (2 meters, Table 2). Lower *Trichodesmium* densities and slick observations were observed in situ in April-May 2002-2003 and October 2001-2003 (Table 1 and 2) which also appear as lower surface bloom extent identified by TRICHOSAT. A surprisingly low *Trichodesmium* concentration (200-400 trichomes.L⁻¹) was observed in the water column in December 2001-January 2002 compared to 2002 and 2003 February months. In June-August 2003 (winter season), *Trichodesmium* was rare and total chlorophyll in the > 10 µm fraction was less than 10% (Table 2). Thus, the community was dominated by picoplankton (cyanobacteria and picoeucaryotes) and surface bloom extent detected by TRICHOSAT was minimum.

The number of selected pixels by TRICHOSAT is however small. It corresponds to surface blooms, occurring in summer, which occupy a large area according to ocean color maps and to field observations. These surface blooms correspond to a physiological state where colonies become buoyant because they cannot synthesize ballast anymore due to phosphate limitation in; colonies thus float as dead material and accumulate at the surface (Moutin et al., 2005). Such conditions may be spatially and temporally de-coupled from sub-bloom *Trichodesmium* concentrations and may not correspond to actively growing *Trichodesmium* colonies. So, the global estimation of dinitrogen fixation by TRICHOSAT remains to be estimated.

Last, the relative abundance of *Trichodesmium* and other nitrogen-fixing cyanobacteria needs to be determined. Coccoid cyanobacteria (*Chrocosphaera*, *Cyanothece*) have been detected from their phycoerythrin signature (Neveux et al., 2006) and flow cytometric properties in the SP (Neveux, unpublished res.; Campbell et al., 2006; Moisander et al., 2010; Sato et al., 2010; Biegala, pers. com.). Nitrogen-fixing heterotrophic bacteria have also been identified in the SP (Rieman et al., 2010). During summer, nitrogen fixation both from filamentous and coccoid cyanobacteria (Garcia et al., 2007; Hynes et al., 2009) experienced high rates (151-703 µM N₂ m⁻² d⁻¹) compared to rates measured at the North of Papua-New

Guinea (Bonnet et al., 2009). Late 2007 field observations confirmed the dominance of *Trichodesmium* in association with *Crocosphaera* in the South Pacific, spatially decoupled from unicellular cyanobacteria (Hewson et al., 2009; Moisander et al., 2010; Sato et al., 2010). *Crocosphaera*, *Cyanothece* and picocyanobacteria populations may form a high fraction of total nitrogen fixation which will not be detected by TRICHOSAT. Applications of the algorithm for an estimate of potential nitrogen fixation would require a better understanding of the relationship between the development of *Trichodesmium* over the whole water column and surface accumulations. Furthermore, a better knowledge of the spatial and temporal association of coccoid cyanobacteria with *Trichodesmium* (Campbell et al., 2006; Sato et al., 2010; Moisander et al., 2010), would help in getting a global view of all nitrogen fixing organisms.

5. CONCLUSION

The TRICHOSAT algorithm is efficient at discriminating *Trichodesmium* surface accumulations in the Western tropical Pacific Ocean. Its results can complement the identification of major functional groups provided by PHYSAT. TRICHOSAT was developed for the SP and is even able to follow the daily evolution of surface blooms over the whole 1998-2010 period (Figure 10). Its application at a global scale requires that the RAS criteria in TRICHOSAT is representative of *Trichodesmium* blooms in other regions, and also that surrounding waters characteristics resemble those in the SP. Reasons why detection of *Trichodesmium* with other algorithms was much less successful (100 times less pixels and no seasonality) in the Western Tropical Pacific Ocean may be, 1) low *Trichodesmium* concentrations, 2) a weak discriminating optical signal such as that due to a mixed optical assemblage, and 3) a significantly different *Trichodesmium* optical signature in the SP.

Trichodesmium experienced a high inter-annual variability in the region with maxima in 1999, 2003, 2004 and 2005, while 2001 and 2002 were less favourable. This inter-annual variability might be related to large scale circulation dynamics. For example, the bifurcation latitude of the South Equatorial Current is found to move southward from about 15°S near the surface to south of 22°S in the intermediate layers (Qu and Lindstrom, 2002) associated with large scale changes in the phosphate pool (Dyrhman et al., 2006; Tadokoro et al., 2009). Also, iron-rich dust deposition patterns (Gao et al., 2001) may be highly variable. Whether other phytoplankton blooms are triggered by *Trichodesmium* decomposition of organic matter is

also of interest (Chen et al., 2008; 2011). Late summer chlorophyll blooms in the oligotrophic North Pacific subtropical gyre may be fuelled by *Trichodesmium* (Wilson and Qiu, 2008).

TRICHOSAT demonstrated that *Trichodesmium* blooms are a common feature in the SP during austral summer (October to March). They are temporally and spatially linked to diverse nitrogen-fixing populations and can be identified as a major potential carbon sink in the SP. A large-scale physical and biogeochemical modeling of the distribution of *Trichodesmium* is required in the SP.

ACKNOWLEDGEMENTS

The authors are grateful to all Commandants of the French Navy in New Caledonia over the 1998-2010 period for aerial and ship observations, and Commandants of Vessels ‘*La Glorieuse*’, ‘*La Moqueuse*’, and the Batral ‘*Jacques Cartier*’ as well as the French Navy based at La Tontouta Airport aeronaval basis for airplane observations. We also thank Raymond Proner et Hervé Le Houarno, Jean-François Barazer, as well as the crew of the RV ‘*Alis*’ for their shipboard support during the operations at sea and observations. We thank Guillaume Dirberg for participation in the MOTEVAS cruise and for photography at the microscope in the laboratory of our colleague Guy Cabioch (LOCEAN, Paris) allowing identifications of morphotypes. Thanks to Alain Lapetite for his help in collecting sea samples and to all observers, Isabelle Biegala, Jean-Yves Panché, and Francis Gallois, Jean-Louis Laurent, Michel Lardy, Stéphane Calmant, Jean-Michel Boré, students Xavier Combres, Romain Charraudeau, Philippe Borsa, Céline Chauvin, and Guillaume Dirberg for their kindly help during cruises despite bad weather conditions. Thanks to Marcio Tenório for biomass measurements and cell counts during the Diapalis cruises. This work would not have been possible without the constant support by Aubert Le Bouteiller, Chief scientist of the Diapalis cruises on the R/V ‘*Alis*’ and of the DIAPAZON (DIAzotrophy PACific ZONE, 2001-2003) program. “Giovanni”, an easy-to-use, Web-based interface for the visualization and analysis of Earth Science data provided by the GES DISC DAAC, the data used in this effort were acquired as part of the activities of NASA's Science Mission Directorate, and are archived and distributed by the Goddard Earth Sciences (GES) Data and Information Services Center (DISC). Finally, we thank NASA for the MODIS real-time observation (Acker and Lepthouck, 2007) web site <http://earthobservatory.nasa.gov/IOTD/view.php?id=46954>) and Image Science and Analysis Laboratory, NASA-Johnson Space Center "The Gateway to Astronaut Photography of Earth.

1 This work was supported by the Institut de Recherche pour le Développement (IRD), the
2 Institut National des Sciences de l'Univers (INSU) and by the French program PROOF
3 (PROcessus biogéochimiques dans l'Océan et Flux). We thank the Ocean Biology Processing
4 Group "Sea-viewing Wide Field-of-view Sensor Project" and particularly Gene Feldman at
5 the Goddard Space Flight Center of NASA (USA).
6

7 REFERENCES

- 8 Acker, J. G. and Leptoukh, G.: Online Analysis Enhances Use of NASA Earth Science Data,
9 Eos, Trans. AGU, Vol. 88(2), p. 14, p. 17, 2007.
- 10 Alvain, S., Moulin, C., Dandonneau, Y., and Breon, F. M.: Remote sensing of phytoplankton
11 group in case 1 waters from global SeaWiFS imagery, Deep-Sea Res. Pt I, 52, 1989-2004,
12 2005.
- 13 Barcelos e Ramos, J., Biswas, H., Schulz, K.G., LaRoche, J., and Riebesell, U.: Effect of
14 rising atmospheric carbon dioxide on the marine nitrogen fixer *Trichodesmium*. Global
15 Biogeochemical Cy., 21, GB2028, doi:10.1029/2006GB002898, 2007.
- 16 Bell, P. R. F., Elmetri, I., and Uwins, P.: Nitrogen fixation by *Trichodesmium* spp. in the
17 Central and Northern Great Barrier Reef Lagoon: relative importance of the fixed-nitrogen
18 load. Mar. Ecol. -Prog. Ser., 186, 119-126, 1999.
- 19 Berman-Frank, I., Bidle, K. D., Haramaty, L., and Falkowski, P. G.: The demise of the marine
20 cyanobacterium, *Trichodesmium* spp., via an autocatalyzed cell death pathway. Limnol.
21 Oceanogr., 49, 997-1005, 2004.
- 22 Bonnet, S., Biegala, I. C., Dutrieux, P., Slemons, L. O., and Capone, D. G.: Nitrogen fixation
23 in the western equatorial Pacific: rates, diazotrophic cyanobacterial size class distribution,
24 and biogeochemical significance. Global Biogeochem. Cy., 23, 1-13, 2009.
- 25 Bowman, T. E., and Lancaster, L. J.: A bloom of the planktonic blue-green alga,
26 *Trichodesmium erythraeum*, in the Tonga Islands. Limnol. Oceanogr., 10, 291-293, 1965.
- 27 Bracher, A., Vountas M., Dinter, T., Burrows, J. P., Röttgers, R., and Peeken, I.: Quantitative
28 observation of cyanobacteria and diatoms from space using PhytoDOAS on
29 SCIAMACHY data, Biogeosciences, 6, 751-754, doi:10.5194/bg-6-751-2009, 2009.
- 30 Breitbarth, E., Oschlies, A., and LaRoche, J.: Physiological constraints on the global
31 distribution of *Trichodesmium*: effect of temperature on diazotrophy, Biogeosciences, 4,
32 53-61, doi:10.5194/bg-4-53-2007, 2007.

- Bryan, S. E., Cook, A., Evans, J. P., Colls, P. W., Wells, M. G., Lawrence, M. G., Jell, J. S., Greig, A., Leslie, E.: Pumice rafting and faunal dispersion during the 2001-2002 in the Southwest Pacific: record of a dacitic submarine explosive eruption from Tonga. *Earth Plan. Sci. Lett.*, 227, 135-154, 2004.
- Campbell, L., Carpenter, E. J., Montoya, J. P., Kustka, A. B., and Capone, D.G.: Picoplankton community structure within and outside a *Trichodesmium* bloom in the southwestern Pacific Ocean. *Vie Milieu*, 55, 185-195, 2006.
- Capone, D. G. and Knapp, A. N.: Oceanography, A marine nitrogen cycle fix? *Nature*, 445, 159-160, doi:10.1038/445159A, 2007.
- Capone, D. G., Zehr, J. P., Paerl, H. W. , Berman, B., and Carpenter, E. J.: *Trichodesmium*, a globally significant marine cyanobacterium. *Science*, 276, 1221-1229, 1997.
- Capone, D. G., Burns, J.A., Montoya, J. P., Subramaniam, A., Mahaffey, C., Gunderson, T., Michaels, A.F., and Carpenter E. J.: Nitrogen fixation by *Trichodesmium* spp.: an important source of new nitrogen to the tropical and subtropical North Atlantic Ocean. *Global Biogeochem. Cy.*, 19, GB2024, doi:10.1029/2004GB002331, 2005.
- Carpenter, E. J.: Nitrogen fixation by marine Oscillatoria *Trichodesmium* in the world's ocean. In: *Nitrogen in the Marine Environment*, edited by: Carpenter, E. J. and Capone, D. J., Academic Press, New-York, 65-103, 1983.
- Carpenter, E. J., O'Neil, J. M., Dawson, R., Capone, D. G., Siddiqui, P. J. A., Roenneberg, T., and Bergman, B.: The tropical diazotrophic phytoplankter *Trichodesmium*: biological characteristics of two common species. *Mar. Ecol.-Prog. Ser.*, 95, 295-304, 1993.
- Chen, Y. L. L., Chen H. Y., Tuo S., and Ohki, K.: Seasonal dynamics of new production from *Trichodesmium* N₂ fixation and nitrate uptake in the upstream Kuroshio and South China Sea basin. *Limnol. Oceanogr.*, 53, 1705–1721, 2008.
- Chen, Y. L. L., Tuo, S., and Chen, H.Y.: Co-occurrence and transfer of fixed nitrogen from *Trichodesmium* spp. to diatoms in the low-latitude Kuroshio Current in the NW Pacific. *Mar. Ecol.-Prog. Ser.*, 421, 25-38, 2011.
- Church, M. J., Bjorkman, K. M., Karl, D. M., Saito, M. A., and Zehr, J. P.: Regional distributions of nitrogen fixing bacteria in the Pacific Ocean, *Limnol. Oceanogr.*, 53(1), 63-77, 2008.
- Church, M. J., Mahaffey, C., Letelier, R. M., Lukas, R., Zehr, J. P., and Karl, D. M.: Physical forcing of nitrogen fixation and diazotroph community structure in the North Pacific

1 Subtropical Gyre, Global Biogeochem. Cy., 23, GB2020, doi:10.1029/2008GB003418,
2 2009.

3 Dandonneau, Y. and Gohin, F.: Meridional and seasonal variations of the sea surface
4 chlorophyll concentration in the South western tropical Pacific ocean. Deep-Sea Res., 31,
5 137-139, 1984.

6 Deutsch, C., Sarmiento, J. L., Sigman, D. M., Gruber, N., and Dunne, J. P.: Spatial coupling
7 of nitrogen inputs and losses in the ocean, Nature, 445, doi:10.1038/nature05392, 2007.

8 Devassy, V. P., Bhattathiri, P. M. A., and Qasim, S. Z.: *Trichodesmium* phenomenon, Ind. J.
9 Mar. Sci., 7, 168–186, 1978.

10 Dore, J. E., Letelier, R. M., Church, M. J., Lukas, R., and Karl, D.: Summer phytoplankton
11 blooms in the oligotrophic North Pacific Subtropical gyre: Historical perspective and
12 recent observations, Prog. Oceanogr., 76, 2-38, 2008.

13 Dupouy, C.: La chlorophylle de surface observée par le satellite NIMBUS-7 CZCS autour de
14 la Nouvelle Calédonie et de ses dépendances. Une première analyse. Bulletin de l'Institut
15 Océanographique de Monaco, p. 125-148. Colloque Scientifique Franco-Japonais;
16 Colloque d'Océanographie, 5: 2, Tokyo; Shimizu J. P. N, 3-13 October 1998, 1990.

17 Dupouy, C.: Discoloured waters in the Melanesian archipelago New Caledonia and Vanuatu.
18 The value of the Nimbus-7 Coastal Zone Colour Scanner observations, in: Marine Pelagic
19 Cyanobacteria: *Trichodesmium* and other diazotrophs, edited by Carpenter, E. J., Capone,
20 D. G. and Rueter J. G., Kluwer Academic Press, NATO Adv. Sci. I. C-Mat., 362: 177-
21 191, 1992.

22 Dupouy, C. and Röttgers, R.: Absorption by different components during a high freshwater
23 event of the 2008 La Nina episode in a tropical lagoon. Poster Session “Bio-optics and
24 biogeochemistry”, Ocean Optics XX, Anchorage (Alaska), 25-30 september 2010.

25 Dupouy, C., Petit, M., and Dandonneau, Y.: Satellite detected cyanobacteria bloom in the
26 southwestern tropical Pacific. Implication for oceanic nitrogen fixation. Int. J. Rem.
27 Sens., 9, 389-396, 1988.

28 Dupouy, C., Neveux, J., Subramaniam, A., Mulholland, M., Campbell, L., Montoya, J.,
29 Carpenter, E., and Capone, D.: Satellite captures *Trichodesmium* blooms in the
30 Southwestern Tropical Pacific. EOS Trans. AGU, 81, 13, 14-16, 2000.

31 Dupouy, C., Dirgerg, G., Tenório, M. M. B., Neveux, J., and Le Bouteiller, A.: Surveillance
32 des *Trichodesmium* autour de la Nouvelle-Calédonie, du Vanuatu, de Fidji et de Tonga
33 1998-2004. Archives Sciences de la Mer, 7, 51, 2004a.

- 1 Dupouy, C., Neveux, J., and Le Bouteiller, A.: Spatial and temporal analysis of SeaWiFS sea
2 surface chlorophyll, temperature, winds and sea level anomalies in the South Tropical
3 Pacific Ocean (10°S-25°S, 150°E-180°E). In : Proceedings “6ème conférence PORSEC,
4 Pan Ocean Remote Sensing Conference”, 29 November- 3 December 2004, Guyana,
5 Conception (Chili), Guyana 68(2) Suppl. I. Proc. 161-166, 2004 ISSN 0717-652X, doi:
6 10.4067/S0717-65382004000200030, 2004b.
- 7 Dupouy, C., Neveux J., Dirberg, G., Röttgers, R., Tenório, M. M. B., and Ouillon, S.: Bio-
8 optical properties of the marine cyanobacteria *Trichodesmium* spp., J. Appl. Remote
9 Sens., 2, 1-17. doi:10.1117/1.2839036, 2008.
- 10 Dyrhman, S. T., Chappell, P. D., Haley, S. T., Moffett, J.W., Orchard, E. D., Waterbury, J. B.,
11 and Webb, E. A.: Phosphonate utilization by the globally important marine diazotroph
12 *Trichodesmium*. Nature, 439, 68-71, 2006.
- 13 Falkowski, P.G.: Evolution of the nitrogen cycle and its influence on the biological
14 sequestration of CO₂ in the ocean, Nature, 387, 272-275, 1997.
- 15 Feldman, G. C. and McClain C. R.: Ocean Color Web, edited by: Kuring, N., Bailey, S. W.,
16 Franz, B. F., Meister, G., Werdell, P. J., and Eplee, R. E., NASA Goddard Space Flight
17 Center, 2010.
- 18 Furnas, M. J.: Cyclonic disturbance and a phytoplankton bloom in a tropical shelf ecosystem,
19 in: Red tides: Environmental Science and Toxicology, edited by: Okaichi, T., Anderson, D.
20 M., and Nemoto, T., Elsevier, Amsterdam, 271-274, 1989.
- 21 Gao, Y., Kaufman, Y.J., Tanre, D., Kolber, D., and Falkowski, P.: Seasonal distributions of
22 aeolian iron fluxes to the global ocean. Geophys. Res. Lett. 28: 29-32, 2001.
- 23 Garcia, N., Raimbault, P., and Sandroni, V.: Seasonal nitrogen fixation and primary
24 production in the southwest Pacific: nanoplankton diazotrophy and transfer of nitrogen to
25 picoplankton organisms. Mar. Ecol.-Prog. Ser. 343:25-33, 2007.
- 26 Gruber, N. and Sarmiento, J. L.: Global patterns of marine nitrogen fixation and
27 denitrification. Global Biogeochem. Cy., 11, 235-266, 1997.
- 28 Hashihama, F., Sato, M., Takeda, S., Kanda, J., and Furuya, K.: Mesoscale decrease of
29 surface phosphate and associated phytoplanktonic dynamics in the vicinity of the
30 subtropical South Pacific Islands. Deep-Sea Res. Pt I, 57, 338-350, 2010.
- 31 Hewson, I., Poretsky, R. S., Dyrhman, S. T., Zielinski, B., White, A. E., Tripp, H. J.,
32 Montoya, J., and Zehr, J. P.: Microbial community gene expression within colonies of the
33 diazotroph, *Trichodesmium*, from the Southwest Pacific Ocean, ISME, 1-15, 2009.

- 1 Hu, C., Cannizzaro, J., Carder, K. L., Muller-Karger, F. E., and Hardy, R.: Remote detection
2 of *Trichodesmium* blooms in optically complex coastal waters: Examples with MODIS
3 full-spectral data, *Remote Sens. Environ.*, 114, 2048-2058, 2010.
- 4 Hutchins, D.A., Fu, F.-X., Zhang, Y., Warner, M.E., Portune, K., Bernhardt, P.W., and
5 Mulholland, M.R.: CO₂ control of *Trichodesmium* N₂ fixation, photosynthesis, growth
6 rates, and elemental ratios: implications for past, present, and future ocean
7 biogeochemistry. *Limnol. Oceanogr.*, 52, 1293–1304, 2007.
- 8 Hynes, A. M., Chappell, P. D., Dyhrman, S. T., Doney, S. C., and Webb, E. A.: Cross-basin
9 comparison of phosphorus stress and nitrogen fixation in *Trichodesmium*. *Limnol.*
10 *Oceanogr.*, 54, 5, 1438-1448, 2009.
- 11 Karl, D. M., Michaels, A., Bergman, B., Capone, D., Carpenter, E., Letelier, R., Lipschultz,
12 F., Paerl, H., Sigman, D., and Stal, L.: Dinitrogen fixation in the world's oceans.
13 *Biogeochemistry*, 57/58, 47-98, 2002.
- 14 Kitajima, S., Furuya, K., Hashihama, F., and Takeda, S.: Latitudinal distribution of
15 diazotrophs and their nitrogen fixation in the tropical and subtropical western North
16 Pacific, *Limnol. Oceanogr.*, 54, 537-547, 2009.
- 17 Konno, U., Tsunogai, U., Komatsu, D. D., Daita, S., Nakagawa, F., Tsuda, A., Matsui, T.,
18 Eum, Y-J., and Suzuki, K., 2010. Determination of total N₂ fixation rates in the ocean
19 taking into account both the particulate and filtrate fractions, *Biogeosciences*, 7, 2369–
20 2377, doi:10.5194/bg-7-2369-2010, 2010.
- 21 Kranz, S., Sültemeyer, D., Richter, K. U., and Rost, B.: Carbon acquisition by
22 *Trichodesmium*: the effect of pCO₂ and diurnal changes. *Limnol. Oceanogr.*, 54, 548-559,
23 2009.
- 24 Kuchler, D. and Jupp, D. L. B.: Shuttle photograph captures massive phytoplankton bloom in
25 the Great Barrier Reef, *Int. J. Remote Sens.*, 9(8), 1299-1301, 1988.
- 26 Kutzer, T.: Passive optical remote sensing of cyanobacteria and other intense phytoplankton
27 blooms in coastal and inland waters, *Int. J. Remote Sens.*, 30(17), 4401-4425, 2009.
- 28 Lantoiné, F. and Neveux, J.: Spatial and seasonal variations in abundance and spectral
29 characteristics of phycoerythrins in the Tropical Northeastern Atlantic Ocean. *Deep-Sea*
30 *Res. Pt I*, 44: 223-246, 1997.
- 31 LaRoche J. and Breitbarth, E.: Importance of the diazotrophs as a source of new nitrogen in
32 the ocean. *J. Sea Res.*, 53, 67-69, 2005.
- 33 Levitan, O., Brown, C. M., B., Sudhaus, S., Campbell, D., LaRoche, J., and Berman-Frank, I.:
34 Regulation of nitrogen metabolism in the marine diazotroph *Trichodesmium* IMS101

under varying temperatures and atmospheric CO₂ concentrations, *Environ. Microb.*, 12, 1899-1912, 2010.

Loisel, H., Nicolas, J. M., Sciandra, A., and Stramski, D.: Spectral dependency of optical backscattering by marine particles from satellite remote sensing of the global ocean”, *J. Geophys. Res.* 111, C09024, doi:10.1029/2005JC003367, 2006.

Lundgren, P., Janson, S., Jonasson, S., Singer, A., and Bergman B.: Unveiling of Novel Radiations within *Trichodesmium* Cluster by *hetR* Gene Sequence Analysis, *App. Environm. Microb.*, 71, 190-196, 2005.

Mahaffey, C., Michaels, A.F., and Capone, D.G.: The conundrum of marine N₂ fixation. *Amer. J. Sci.*, 305: 546-595, 2005.

Mantas, V. M., Pereira, A.J.S.C., Morais, P.V.: P.V. Plumes of discolored water of volcanic origin and possible implications for algal communities. The case of the Home Reef eruption of 2006 (Tonga, Southwest Pacific Ocean). *Remote Sens. Environ.*, 115, 1341–1352, 2011.

Maritorena, S. and Siegel, D. A.: Consistent merging of satellite ocean color data sets using a bio-optical model. *Remote Sensing Environ.*, 94, 429-440, 2005.

Masotti I., Ruiz-Pino, D., and Le Bouteiller, A.: Photosynthetic characteristics of *Trichodesmium* in the southwest Pacific Ocean: importance and significance. *Mar. Ecol.-Prog. Ser.*, 338, 37-49, 2007.

McKinna, L. I.W., Furnas, M. J., and Ridd, P. V.: A simple, binary classification algorithm for the detection of *Trichodesmium* spp. within the Great Barrier Reef using MODIS imagery, *Limnol. Oceanogr. Methods*, 9:50-66 (2011), doi: 10.4319/lom.2010.9.50, 2011.

Moisander, P. H., Beinart, R. A., Hewson, I. White, A. E., Johnson, K. S., and Carlson, C. A.: Unicellular Cyanobacterial Distributions Broaden the Oceanic N₂ Fixation Domain, *Science*, 327, 1512-1514, doi:10.1126/science.1185468, 2010.

Monteiro, F. M., Follows, M. J., and Dutkiewicz, S.: Distribution of diverse nitrogen fixers in the global ocean, *Global Biogeochem. Cy.*, 24, GB3017, doi:10.1029/2009GB003731, 2010.

Montoya, J., Holl, C. M., Zehr, J. P., Hansen, A., Villareal, T. A., and Capone, D. G.: High Rates of N₂ Fixation by Unicellular Diazotrophs in the Oligotrophic Pacific. *Nature*, 430, 1027-1032, 2004.

Moutin, T., Van den Broeck, N., Beker, B., Dupouy, C., Rimmelín, P., and Le Bouteiller, A.: Phosphate availability controls *Trichodesmium* spp. biomass in the SW Pacific Ocean. *Mar. Ecol.-Prog. Ser.*, 207, 15-21, 2005.

- 1 Mulholland, M.: The fate of nitrogen fixed by diazotrophs in the ocean, *Biogeosciences*, 4,
2 37-51, doi:10.5194/bg-4-37-2007, 2007.
- 3 Neveux, J., Lantoine, F., Vaulot, D., Marie, D. and Blanchot, J.: Phycoerythrins in the
4 southern tropical and equatorial Pacific Ocean: Evidence for new cyanobacterial types. *J.*
5 *Geophys. Res.*, 104(C2): 3311–3321, 1999.
- 6 Neveux, J., Tenório, M.M.B., Dupouy, C., and Villareal, T.: Spectral diversity of
7 phycoerythrins and diazotrophs abundance in tropical South Pacific. *Limnol. Oceanogr.*,
8 51, 4, 1689-1698, 2006.
- 9 Qu T. and Lindstrom, E. J.: A climatological interpretation of the circulation in the western
10 south Pacific. *J. Phys. Oceanogr.*, 32, 2492-2508, 2002.
- 11 Ramos, A.G.R., Martel, A., Codd, G.A., Soler, E., Coca, J., Redondo, A., Morrison, L.F.,
12 Metcalf, J.S., Ojeda, A., Duarez, S., and Petit, M.: Bloom of the marine diazotrophic
13 cyanobacterium *Trichodesmium erythraeum* in the Northwest African Upwelling, *Mar.*
14 *Ecol.-Prog. Ser.*, 301, 303-305, 2005.
- 15 Revelante, N. and Gilmartin, M.: Dynamics of phytoplankton in the Great Barrier Reef
16 lagoon. *J. Plankton Res.*, 4, 47-76, 198, 1982.
- 17 Riemann, L., Farnelid, H., and Steward, G.F.: Nitrogenase genes in non-cyanobacterial
18 plankton: prevalence, diversity and regulation in marine waters, *Aquat. Microb. Ecol.*, 61,
19 235–247, doi:10.3354/ame01431, 2010.
- 20 Rubin, M., Berman-Frank, I. and Shaked H. : Dust- and mineral-iron utilization by the marine
21 dinitrogen-fixer *Trichodesmium*. *Nature Geosci.*, 4, 529–534, doi:10.1038/ngeo1181, 2011.
- 22 Sarangi, R.K., Chauhan, P., and Nayak, S. R.: Detection and monitoring of *Trichodesmium*
23 blooms in the coastal waters off Saurashtra coast, India using IRS-P4 OCM data, *Curr.*
24 *Sci.*, 86, 12, 1636-1641, 2004.
- 25 Sato, M., Hashihama, F., Kitajima, S., Takeda, S., and Furuya, K.: Distribution of nano-sized
26 cyanobacteria in the western and central Pacific Ocean, *Aquatic Microb. Ecol.*, 59, 273-
27 282, 2010.
- 28 Shiozaki, T., Furuya, K., Kodama, T., and Takeda, S.: Contribution of N₂ fixation to new
29 production in the western North Pacific Ocean along 155°E, *Mar. Ecol.-Prog. Ser.*, 377,
30 19-32, 2009.
- 31 Siegel, D. A., S. Maritorena, N. B. Nelson, D. A. Hansell, and Lorenzi-Kayser, M.: Global
32 distribution and dynamics of colored dissolved and detrital organic materials, *J. Geophys.*
33 *Res.*, 107(C12), 3228, doi:10.1029/2001JC000965, 2002.

- 1 Siegel, D. A., S. Maritorena, N. B. Nelson, and Behrenfeld, M. J.: Independence and
2 interdependencies of global ocean color properties: Reassessing the bio-optical
3 assumption, J. Geophys. Res., 110, C07011, doi:10.1029/2004JC002527, 2005.
- 4 Subramaniam, A., E. J., Carpenter, D., Karentz, and Falkowski, P.G.: Bio-optical properties
5 of the diazotrophic cyanobacteria *Trichodesmium* spp. I. Absorption and photosynthetic
6 action spectra. Limnol. Oceanogr., 44, 608-617, 1999.
- 7 Subramaniam, A., Brown, C. W., Hood, R. R., Carpenter, E. J., and Capone, D. G.: Detecting
8 *Trichodesmium* blooms in SeaWiFS imagery. Deep-Sea Res. Pt I, 49, 107-121, 2002.
- 9 Tadokoro, K., Ono, T., Yasuda, I., Osafune, S., Shiimoto, A., and Sugisaki, H.: Possible
10 mechanisms of decadal scale variation in PO₄ concentration in the western North Pacific,
11 Geophys. Res. Lett., 36, L08606, doi:10.1029/2009GL037327, 2009.
- 12 Tenório, M. M. B. : Les cyanobactéries en milieu tropical: occurrence, distribution, écologie
13 et dynamique, PhD Thesis, Université Paris VI, 2006.
- 14 Westberry T., Subramaniam, A., and Siegel, D.: An improved bio-optical algorithm for the
15 remote sensing of *Trichodesmium* spp. blooms, J. Geophys. Res., 110, C06012,
16 doi10.1029/2004JC, 2005.
- 17 Westberry, T. K. and Siegel, D. A.: Spatial and temporal distribution of *Trichodesmium*
18 blooms in the world's oceans. Global Biogeochemical Cy., 20, 4016,
19 doi10.1029/2005GB002673, 2006.
- 20 Wilson, C. and X. Qiu, X.: Global distribution of summer chlorophyll blooms in the
21 oligotrophic gyres, Prog. Oceanogr., 78, 107-134, doi:10.1016/j.pocean.2008.05.002,
22 2008.
- 23 Zehr, J. P. and Kudela, R. M.: Nitrogen cycle of the open ocean: from genes to ecosystems,
24 Annu. Rev. Marine Sci., 3, 197-225, 2011.
- 25 Zehr, J. P., Waterbury, J. B., Turner, P. J., Montoya, J. P., Omoregie, E., Steward, G. F.,
26 Hansen, A., and Karl, D. M.: Unicellular cyanobacteria fix N₂ in the subtropical North
27 Pacific Ocean. Nature, 412, 635-638: doi:10.1038/35088063, 2001.

28 .

1

2 **Table 1.** In situ *Trichodesmium* bloom observations for the period 1998-2010 in the South Western Tropical Pacific (NC, New Caledonia). Data
3 from aerial observations, and/or bucket sampling from cruises and various transects made by the French Navy ships and the R/V *Alis*.
4 Abbreviations: T. e., T. t. and T. ten., K., for *Trichodesmium erythraeum*, *thiebautii*, and *tenue*, *Katagnymene* spp., respectively. Col. = colonies;
5 fil. = filaments. Nq s.: nautical miles slicks, shipb.: Shipboard observations. * Ground-truthed (microscopy) aerial or shipboard observations are
6 indicated by an asterisk, ** E. J. Carpenter, personal communication

Year/day/Year	Date	Latitude	Longitude	Observed	Observed	Estimated	Location in the	Observation
				species	form	Slick size	Tropical Pacific	Mean
101/1998**	11 Apr 1998	17° S	179° E	T. t.	large col.	und.	Fiji Isl.	R/V <i>Revelle</i> , NSF
101/1998*	11 Apr 1998	18° S	188° E	T. t.	large col.	und.	Vavau Isl.	F. Navy, <i>J. Cartier</i>
108/1998	18 Nov 1998	22°35' S	168°58' E	und.	und.	nq s.	Walpole Isl.	F. Navy aerial
108/1998	18 Nov 1998	24°21' S	170°40' E	und.	und.	nq s.	SE NC	F. Navy aerial
329/1998	25 Nov 1998	22°15' S	163°35' E	und.	und.	nq s.	W NC	F. Navy aerial
329/1998	25 Nov 1998	21°20' S	164°10' E	und.	und.	nq s.	W NC	F. Navy aerial
329/1998	25 Nov 1998	19°35' S	160°55' E	und.	und.	30 km ²	NW NC	F. Navy aerial
352/1998	18 Dec 1998	22°40' S	165°50' E	und.	und.	nq s.	SW NC	F. Navy aerial
008/1999	8 Jan 1999	23°S	166°E	und.	und.	nq s.	SW NC	F. Navy aerial
008/1999	8 Jan 1999	24°10' S	166°15' E	und.	und.	nq s.	SW NC	F. Navy aerial
008/1999	8 Jan 1999	23°50' S	164°20' E	und.	und.	nq s.	SW NC	F. Navy aerial
313/1999	9 Nov 1999	20° S	170° E	und.	und.	30 km ²	Vanuatu to NC	R/V <i>Alis</i> (Wespalis)
007/2000	7 Jan 2000	21°49' S	165°11' E	und.	und.	nq s.	W NC	F. Navy aerial
007/2000	7 Jan 2000	20°30' S	161°52' E	und.	und.	nq s.	W NC	F. Navy aerial
363/2000	28 Dec 2000	19°57' S	162°58' E	und.	und.	nq s.	Belep	F. Navy aerial
363/2000	28 Dec 2000	21°20' S	164°12' E	und.	und.	nq s.	Poum	F. Navy aerial
363/2000	28 Dec 2000	21°48' S	163°35' E	und.	und.	nq s.	Poum	F. Navy aerial
008/2001	8 Jan 2001	22°20' S	172° E	und.	und.	nq s.	Hunter Isl.	F. Navy aerial

018/2001	18 Jan 2001	21°11' S	164°17' E	und.	und.	nq s.	NW Kone, NC	F. Navy aerial
018/2001*	18 Jan 2001	18°31' S	164°28' E	T. e., T. t., T. Ten.	large col., green	nq s.	Petri Reefs	F. Navy aerial
23/2001*	23 Jan 2001	22°11' S	161°79' E	T. e.	Isolated fil.	nq s.	Coral Sea	F. Navy aerial
23/2001*	23 Jan 2001	22°10' S	161°79' E	T. e.	flocks	Shipb.	Coral Sea	F. Navy, <i>La Moqueuse</i>
29/2001	29 Jan 2001	24°53' S	161°40' E	und.	flocks	Shipb.	Coral Sea	F. Navy, <i>La Moqueuse</i>
29/2001	29 Jan 2001	24°47' S	162°37' E	und.	flocks	Shipb.	Coral Sea	F. Navy, <i>La Moqueuse</i>
125/2001*	7 May 2001	20°12' S	163°29' E	T. e.	green col.	nq s.	Belep	F. Navy aerial
248/2001	5 Sep 2001	20°08' S	170°45' E	und.	und.	nq s.	Anatom	F. Navy aerial
248/2001	5 Sep 2001	20°41' S	170°16' E	und.	und.	nq s.	Anatom	F. Navy aerial
295/2001*	22 Oct 2001	22°16' S	167°27' E	T. e., T. t., K.	flocks	Shipb.	E NC	R/V <i>Alis</i> (Diapalis 1)
285/2001*	3 Nov 2001	20°47' S	167°03' E	T. e.	grey col.	nq s.	Lifou Isl.	F. Navy aerial
317/2001*	13 Nov 2001	22°09' S	167°19' E	T. e., T. t., K.	und.	nq s.	East Coast	F. Navy, <i>La Glorieuse</i>
317/2001*	13 Nov 2001	22' S	167°29' E	T. e., T. t., K.	und.	nq s.	Loyalty Channel	F. Navy, <i>La Moqueuse</i>
030/2002*	30 Jan 2002	22°22' S	166°50' E	T. e.	green col.	nq s.	Uitoe Pass.	F. Navy aerial
030/2002	30 Jan 2002	22°12' S	166°01' E	und.	und.	nq s.	Uitoe Pass.	F. Navy aerial
039/2002	8 Feb 2002	21°26' S	162°32' E	und.	und.	nq s.	Chesterfields Isl.	R/V <i>Alis</i>
111/2002*	21 Apr 2002	23°29' S	162°53' E	T. e.	orange col.	Shipb.	SW NC	F. Navy, J. Cartier
111/2002*	24 Apr 2002	22°28' S	169°12' E	T. e.	pink col.	Shipb.	E Walpole Isl.	F. Navy, J. Cartier
189/2002*	8 Jul 2002	19°08' S	176°41' W	T. e.	grey col.	Shipb.	Fiji Isl.	F. Navy, J. Cartier
197/2002	16 Jul 2002	23°03' S	164°42' E	und.	und.	Shipb.	W NC	F. Navy, <i>J. Cartier</i>
344/2002*	10 Dec 2002	18°40' S	168°59' E	K. + T. e. + T. t.	large col.	nq s.	Erromango Isl.	F. Navy, J. Cartier
345/2002	11 Dec 2002	20°05' S	167°30' E	und.	und.	Shipb.	E Lifou Bay	visual obs
346/2002*	12 Dec 2002	19°19' S	164°51' E	T. e. + K.	green, grey, pummices	Shipb.	Surprises Isl.	F. Navy, <i>La Glorieuse</i>
347/2002*	13 Dec 2002	19°07' S	167°20' E	K. + T. e. + T. t.	large col.	Shipb.	Erromango Isl.	F. Navy, <i>J. Cartier</i>
350/2002*	16 Dec 2002	20°48' S	170°09' W	T. ten., K.	grey, long thin fil.	Shipb.	Niue Isl.	R/V <i>Alis</i>
350/2002*	16 Dec 2002	20°51' S	170°33' W	T. ten., K.	grey, long thin fil.	Shipb.	Niue Isl.	R/V <i>Alis</i>

352/2002*	18 Dec 2002	21°11' S	174°08' W	T. ten., K.	grey, long thin fil.	Shipb.	Niue Isl.	R/V <i>Alis</i>
352/2002*	18 Dec 2002	21°11' S	173°57' W	T. ten., K.	grey, long thin fil.	Shipb.	Niue Isl.	R/V <i>Alis</i>
359/2002	25 Dec 2002	20°11' S	169°04' E	und.	und.	und.	W Tanna Isl.	shipboard
038/2003*	5 Feb 2003	21 °S	166°30' E	T.e.	Brown col.	Shipb.	E NC Loyalty Channel	R/V <i>Alis</i> (Diapalis 07)
048/2003	17 Feb 2003	23°14' S	165°29' E	und.	und.	nq s.	Santo Isl.	F. Navy aerial
051/2003	20 Feb 2003	15°04' S	166°30' E	und.	und.	nq s.	W NC	F. Navy aerial
087/2003*	28 Mar 2003	24°44' S	163°21' E	T. e.	pink col.	Shipb.	S NC	F. Navy, J. Cartier
115/2003	25 Apr 2003	17°57' S	168°10' E	und.	und.	Shipb.	Efate Isl.	F. Navy, <i>J. Cartier</i>
303/2003	30 Oct 2003	14°50' S	168° E	und.	und.	Shipb.	Bank Isl.	ship of opportunity
308/2003*	4 Nov 2003	17°39' S	167°33' E	T. e.	red col.	Shipb.	Vanuatu	F. Navy, <i>La Moqueuse</i>
309/2003	5 Nov 2003	20° S	166°30' E	und.	und.	Shipb.	Ouvea Isl.	visual obs
343/2003	9 Dec 2003	20°24' S	167°51' E	und.	und.	300 km ²	500 km Lifou-Vanuatu	R/V <i>Alis</i>
352/2003	18 Dec 2003	24°03' S	168°02' E	und.	und.	Shipb.	SE NC	F. Navy, <i>La Glorieuse</i>
017/2004	17 Jan 2004	23°20' S	168°20' E	und.	und.	Shipb.	SE NC	F. Navy
023/2004	23 Jan 2004	20°16' S	161° E	und.	und.	Shipb.	NW NC	F. Navy
026/2004*	26 Jan 2004	22°11' S	167°22' E	T. e.	small orange col.	Shipb.	Loyalty Channel	F. Navy, <i>La Glorieuse</i>
029/2004*	29 Jan 2004	20°20' S	166°07' E	T. e.	Large pink flocks	nq s.	Beautemps-Baupré	R/V <i>Alis</i> (PIL)
030/2004*	30 Jan 2004	20°17' S	166°17' E	T. e.	Large pink flocks	nq s.	NE NC	R/V <i>Alis</i> (PIL)
032/2004*	1 Feb 2004	21°20' S	167°35' E	T. e.	Large pink flocks	nq s.	NE NC, Oua Isl.	R/V <i>Alis</i> (PIL)
043/2004	12 Feb 2004	18°30' S	166°30' E	und.	und.	nq s.	W Vanuatu	F. Navy aerial
044/2004	13 Feb 2004	19°50' S	169°54' E	und.	und.	Shipb.	N NC Balabio Isl.	French Navy
047/2004	16 Feb 2004	18°49' S	168°30' E	und.	und.	km s.	500 km NC-Vanuatu	Air Vanuatu
059/2004*	28 Feb 2004	21°10' S	168°30' E	T. e.	orange col.	Shipb.	NE NC coast	R/V <i>Alis</i> (Motevas)
059/2004*	28 Feb 2004	20°52' S	165°57' E	T.e.	brown col.	Shipb.	NE NC coast	R/V <i>Alis</i> (Motevas)
060/2004*	29 Feb 2004	18°33' S	166°03' E	T. t. + K.	floating flocks green tufts long	Shipb.	Vanuatu	R/V <i>Alis</i> (Motevas)
060/2004*	29 Feb 2004	18°20' S	166°02' E	T. t. + K.	fil.	Shipb.	Vanuatu	R/V <i>Alis</i> (Motevas)

060/2004*	29 Feb 2004	17°23' S	166°04' E	T. t. + K.	large puffs/tufts, flocks	Shipb.	Vanuatu	R/V <i>Alis</i> (Motevas)
061/2004*	1 Mar 2004	22° S	167° E	T. e.	White col.	Shipb.	Yate Barrier Reef	F. Navy
064/2004	4 Mar 2004	20°09' S	168°43' E	und.	und.	nq s.	Vanuatu	F. Navy aerial
089/2004	29 Mar 2004	17° S	167° E	und.	und.	nq s.	Masquilignes Isl. N Vanuatu	Air Vanuatu
117/2004	26 Apr 2004	20°09' S	163°01' E	und.	und.	nq s.	Aircraft	F. Navy aerial
275/2004	1 Oct 2004	21°30' S	165' E	und.	und.	nq s.	Lifou	F. Navy aerial
316/2004	11 Nov 2004	18°30' S	168' E	und.	und.	nq s.	Vanuatu	F. Navy aerial
347/2004	12 Dec 2004	22°29' S	169°50' E	und.	und.	nq s.	E Pine Isl. , Walpole Isl.	F. Navy aerial
033/2005*	2 Feb 2005	20° 07' S	170° W	T. e. +T. t. + T. Cont.	und.	und.	East Tonga Isl.	Hashihima et al., 2010
040/2005*	9 Feb 2005	18° 02' S	175° E	T. e. +T. t. + T. Cont.	und.	und.	W Fiji Isl.	Hashihima et al., 2010
090/2007*	30 Mar 2007	22° 49' S	169° 59' E	T. e. + K. + T. C.	Floating puffs	Shipb.	Walpole Isl.	R/V <i>Kilo Moana</i> cruise
089/2007*	8 Apr 2007	15° S	169° 59' W	T. e. + K. + T. C.	Floating puffs	Shipb.	N. Fiji Isl.	R/V <i>Kilo Moana</i> cruise
102/2007*	12 Apr 2007	14° 59' S	178° 45' E	T. e. + K. + T. C.	Surface Bloom	Shipb.	North East Fiji	R/V <i>Kilo Moana</i> cruise
062/2010*	3 Mar 2010	19°11' S	166°57' E	T. e.	orange col.	nq s.	Beautemps- Beaupré Reef	F. Navy aerial
062/2010*	3 Mar 2010	19°06' S	166°07' E	T. e.	orange col.	nq s.	Beautemps- Beaupré Reef	F. Navy, <i>J. Cartier</i>
102/2010	12 Apr 2010	22°48' S	165°17' S	und.	und.	Shipb.	W NC	Ship obs
102/2010	12 Apr 2010	22°06' S	165°26' E	und.	und.	Shipb.	idem	Ship obs
141/2010*	21 May 2010	15°19' S	166°30' E	T. e.	orange col.	Shipb.	Sabine Bank	R/V <i>Alis</i> (Geodeva4)
300/2010	27 Oct 2010	19° S	165°30' E	und.	und.	Shipb.	W NC	Ship obs
301/2010	28 Oct 2010	22° S	167° E	und.	und.	Shipb.	W NC	Ship obs
307/2010*	3 Nov 2010	19°15' S	166°47' E	T. e.	orange col.	Shipb.	SE Vanuatu	F. Navy, R/V <i>Prairial</i>
307/2010*	3 Nov 2010	19°27' S	166°52' E	T. e.	orange col.	Shipb.	SE Vanuatu	F. Navy, R/V <i>Prairial</i>
339/2010	4 Dec 2010	22°12' S	169°42' E	und.	und.	nq s.	SE NC	F. Navy aerial
339/2010	4 Dec 2010	21°26' S	167°19' E	und.	und.	nq s.	W NC	F. Navy aerial
339/2010	4 Dec 2010	22°12' S	167°42' E	und.	und.	nq s.	W NC	F. Navy aerial

1 **Table 2.** Average in situ observations at the surface layer (3 meters Niskin bottle) of filamentous cyanobacteria during the DIAPAZON Program
2 from Tenório (2006), the Motevas cruise, and in surface bucket samples during the transects made on the French Navy ships from New
3 Caledonia to Tr1: Vanuatu, Tr2: Walpole, Tr 3: Vanuatu, Tr 4: Vanuatu, Tr 5: Fiji, Vanuatu, Tr6: Wallis and Futuna and Vanuatu. Tchl a =
4 chlorophyll a + divinyl chlorophyll a ; PE = phycoerythrin; chl > 10 = percentage of Tchl a associated with the > 10 μm fraction, Cp= attenuation
5 coefficient (m^{-1}). Und: undetermined. * E. J. Carpenter, personal communication, ** 1000 in a slick North of Lifou.

Yearday	date	cruise	Tchl- a	PE	Chl > 10	Beam attenuation	Trich. Ab.	Bloom obs
	DD/MM/YY	name	(mg.m^{-3})	(mg.m^{-3})	(%)	(m^{-1})	(Trichomes.L $^{-1}$)	
105/1998	15-Apr-98	Trichonesia	0.14	und.	20	und.	298 (10000 Fiji Isl.)*	Shipboard
295-304/2001	22-31 Oct 01	Diapalis01	0.14	0.16	16	und.	411	Shipboard
344-356/2001	10-22 Dec 01	Diapalis02	0.13	0.15	10	0.072	474	no
15-22/2002	15-22 Jan 02	Diapalis03	0.1	0.09	8.8	0.062	401	no
92-99/2002	2-9 Apr 02	Diapalis04	0.11	0.1	9	0.059	347	no
133-144/2002	13-14 May 02	Transect 1	0.26	0.83	und.	und.	und.	no
141-148/2002	21-28 May 02	Diapalis05	0.11	0.23	9.3	0.046	300 (1000 **)	no
217-224/2002	5-12 Aug 02	Diapalis06	0.22	0.19	9	0.069	76	no
34-43/2003	3-12 Feb 03	Diapalis07	0.23	0.6	53	0.1	> 6000	Shipboard
59/2003	28-Feb-03	Transect 2	0.29	0.45	und.	und.	und.	und.
71-80/2003	12-21 Mar 03	Transect 3	0.29	0.33	und.	und.	und.	und.
107-115/2003	17-25 Apr 03	Transect 4	0.21	0.53	und.	und.	und.	no
112-115/2003	22-25 Apr 03	Transect 5	0.18	0.44	und.	und.	und.	no
161-165/2003	9-14 Jun 2003	Diapalis08	0.2	0.25	7	0.051	300	no
188-208/2003	7-27 Jul 03	Transect 6	0.25	0.09	und.	und.	und.	no
281-289/2003	8-16 Oct 03	Diapalis09	0.099	0.08	9	0.057	9	no
	28-29 Feb 04	Motevas	0.48	0.37	70	und.	4000	Shipboard
59-60/2004	(Niskin)							
	28-29 Feb 04	Motevas	0.84	3.4	70	und.	6500	Shipboard
59-60/2004	(Bucket)							

FIGURE LEGENDS

Fig. 1. (a) Situation map showing limits of the Western Pacific ocean (WP: 25°N-25°S/160°E-160°W) and of the Southern Pacific Ocean box (SP: 5°S-25°S/150°E-190°E/170°W). (b) Mean SeaWiFS composite image of chlorophyll a (mg m^{-3}) in the South Western Tropical Pacific Ocean in February 2003 (austral Summer) with observations of *Trichodesmium* surface accumulations for December 2002-March 2003. Main lands are indicated in yellow (New Caledonia, 20-22°S, 165°E), Vanuatu (15-20°S, 168°E), Fiji (17°S, 180°E) and South Tonga Islands (21°S, 175°W). (c) French Navy observations of *Trichodesmium* surface blooms (1998-2010) from Table 1 as empty black circles, with: light blue - aerial observations; red - small form filaments (named *T. erythraeum* spp. after Tenório, 2006); magenta - mix of small *T. erythraeum* and long forms (filaments of *Trichodesmium thiebautii* and *T. tenue*); yellow - mix of *T. tenue* and *Katagnymene* sp.

Fig. 2. Selected pictures of the January-February 2004 *Trichodesmium* slick as seen from long line airplanes (aerial observation), and from the ship of the French Navy La Glorieuse (shipboard observation with bucket sample) gathered at Table 1.

Fig. 3 (a) Descriptive parameters to characterize the SeaWiFS radiance anomaly spectra relative to K490 for *Trichodesmium* detection in surface oceanic waters: S = slope of the linear fit; Yt = ordinate of the second degree fit for which tangent is parallel to linear fit; “Bump” and “Trough” are the wavelengths of the major positive and major negative deviations relative to the second degree polynomial fit (largest “bump” or largest “trough”, respectively) (b) Ranges of S and Yt for all RAS of all pixels (black). In orange, specific S and Yt and positions of bumps and troughs schematically shown for RAS of a *Trichodesmium* bloom.

Fig. 4. Application of the TRICHOSAT algorithm to satellite data (1997 to 2010) over the large box corresponding to the Western Pacific Ocean (WP: 25°N-25°S/160°E-160°W) for the interseason (April-May and October) (a) all pixels for which $\text{Chl}_a > 0.2 \text{ mg m}^{-3}$; (b) pixels satisfying the slope and intercept criteria of the RAS; (c) pixels satisfying the shape criteria, (d) pixels satisfying all criteria. The main islands of New Caledonia at 20°S, Vanuatu at 15°S, Fiji Islands at 17°S, Hawaii Islands at 20°N are indicated in black Fig. 4d.

Fig. 5. Statistics of the number of SeaWiFS Level_2 GAC images used to determine the spatio-temporal distribution of *Trichodesmium* accumulations in the SP between 1997 and 2010 by year and season. Seasons are defined as: austral summer (November to March); austral winter (June to September); interseason (April-May and October);

Fig. 6. Application of the TRICHOSAT algorithm to satellite data (1997 to 2010) over the large box corresponding to the Western Pacific Ocean (WP: 25°N-25°S/160°E-160°W); **a**): austral winter (June to September); **b**) interseason (April-May and October); **c**) austral summer (November to March). The main islands of New Caledonia at 20°S, Vanuatu at 15°S, Fiji Islands at 17°S, Hawaii Islands at 20°N are indicated in grey.

Fig. 7. (top) Monthly percentage of valid pixels identified as *Trichodesmium* when applying the TRICHOSAT algorithm to SeaWiFS Level-2 imagery (4 km x 4 km). Results are shown for the Southern Pacific Ocean box (SP: 5°S-25°S, 150°E-190°E/170°W) in red and for the WP (WP: 25°N-25°S/160°E-160°W) as black. *Trichodesmium* blooms occur regularly during the austral summer and peak in February. SeaWiFS chlorophyll-*a* for SP also shown as green line (note that the monthly chlorophyll is smoothed compared to chlorophyll concentrations in pixels of individual level2-GAC images) (bottom) GSM-derived ACDM absorption coefficient (m^{-1}) (grey line) and scaled particulate backscattering coefficient (m^{-1}) (dark blue line).

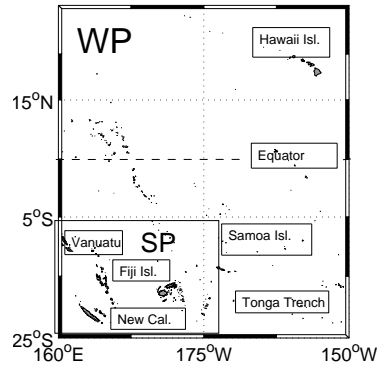
Fig. 8. a) Histogram representing the mean annual cycle of *Trichodesmium* bloom pixels percentage (with standard deviation) over the 12 years (1998-2010) of the SeaWiFS acquisition period; **b)** Histogram representing the mean annual number of in situ slicks observations (Nb, from Table 1).

Fig. 9. Spatial distributions of *Trichodesmium* bloom pixels retrieved with TRICHOSAT in the SP box (5°S- 25°S 160°-170°W) for short periods **(a)** during Austral summer, 10- 22 February 2003 (In Yellow: 2003, 40 (9 Feb), in Magenta: 2003, 42 - 43 (11-12 Feb), in Blue: 2003, 44 - 45 (13-14 Feb), in Red : 2003, 47 - 48 (16-17 Feb), in Green: 2003, 49 - 50 (18-19 Feb) Black: 2003, 52 (21 Feb) and **(b)** during Austral winter, 9 - 15 June, 2003 (Magenta: 2003, 160 (June 9) Blue: 2003, 162 (June 11) Red: 2003, 163 (June 13) Green: 2003, 165 (June 15). The two aerial observations from Table 1 are added. Each pixel represents a surface

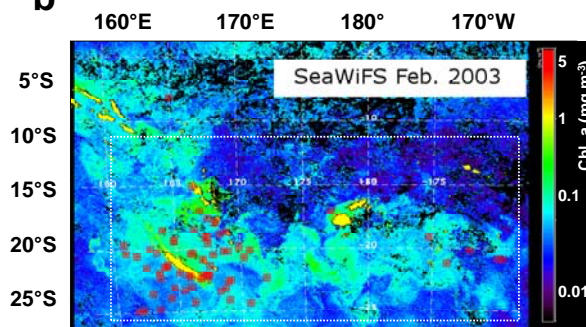
of 16 km² (the size of colored squares is equivalent to a surface of 256 km², i.e. 16 "real" SeaWiFS pixels of 4x4 km). Also shown are results obtained from [Westberry et al. \(2005\)](#) (black crosses) for the same time periods. In grey, the main lands of New Caledonia at 20°S, Vanuatu at 15°S and Fiji Islands at 17°S.

Fig. 10. Daily evolution of the TRICHOSAT retrievals percentage shown as red bars (in % pixels, over the SP domain) from individual SeaWiFS Level_2 GAC images, and number of surface slicks observed per month (Nb issued from Table 1) as black open circles in the SP area for the period 1998-2010.

a Figure 1



b



c

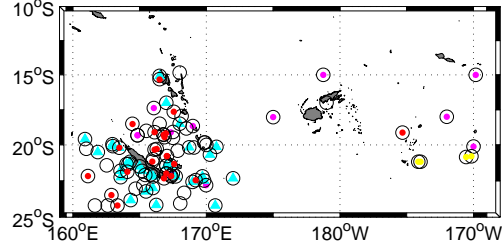


Figure 2

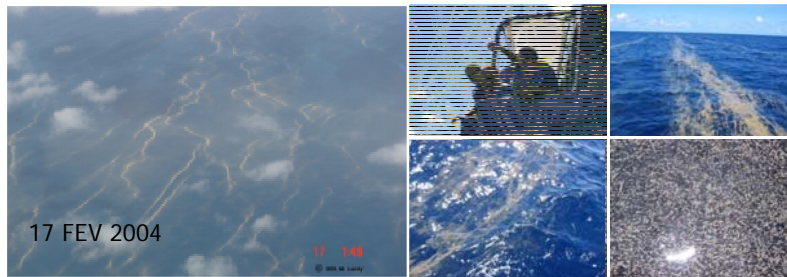


Figure 3ab

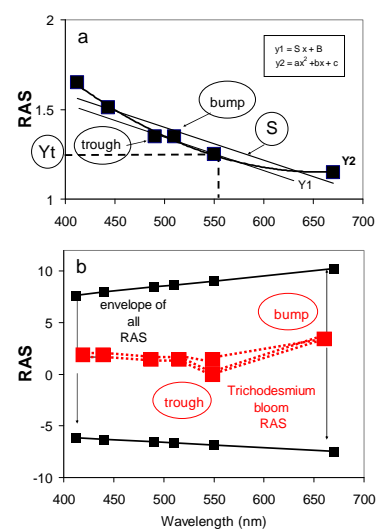


Figure 4abcd

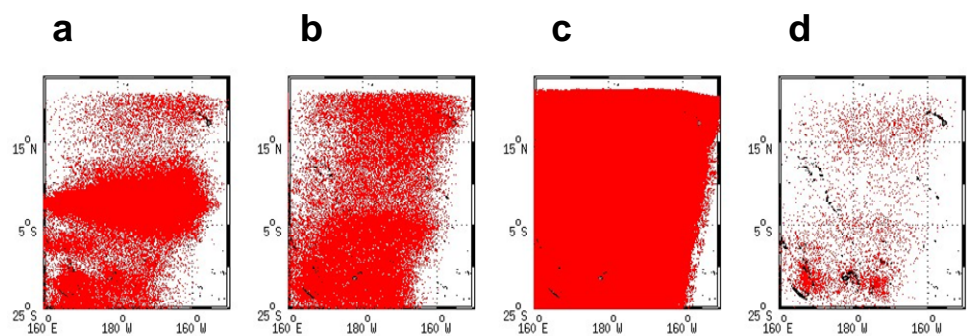


Figure 5

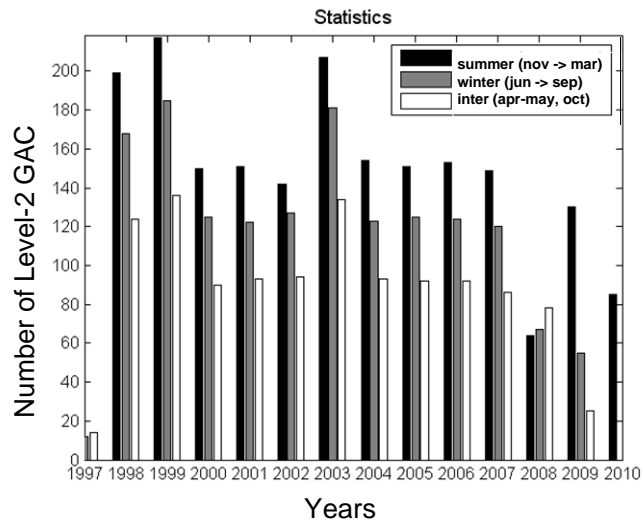


Figure 6

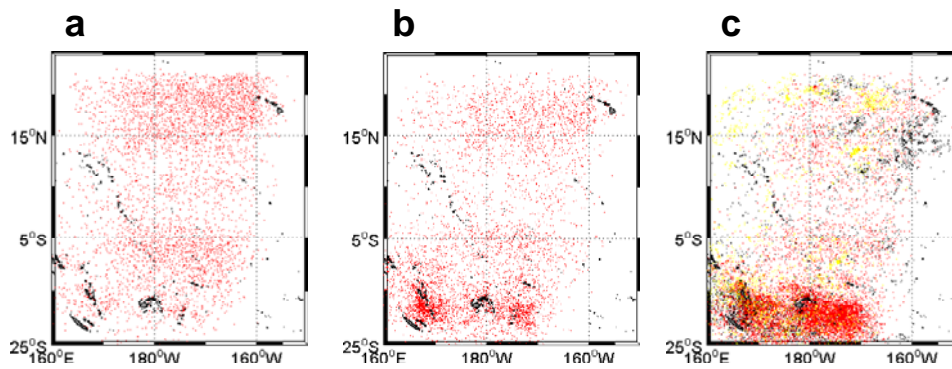
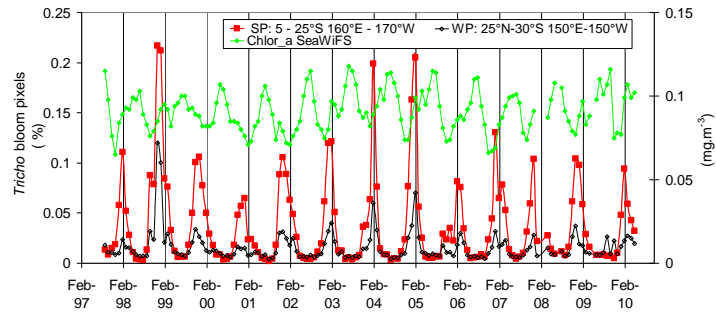


Figure 7

(top)



(bottom)

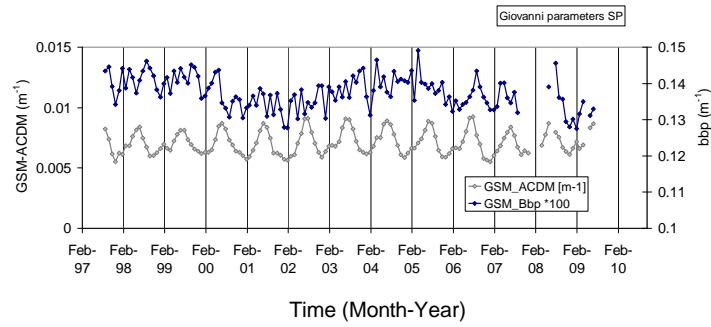
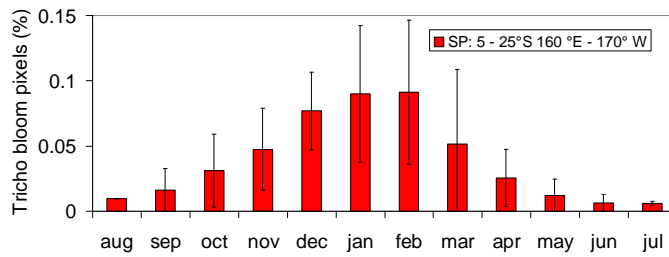
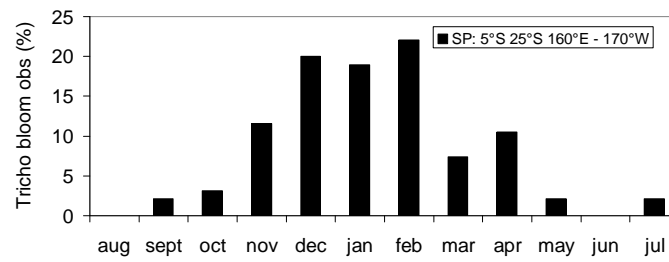


Figure 8

a



b



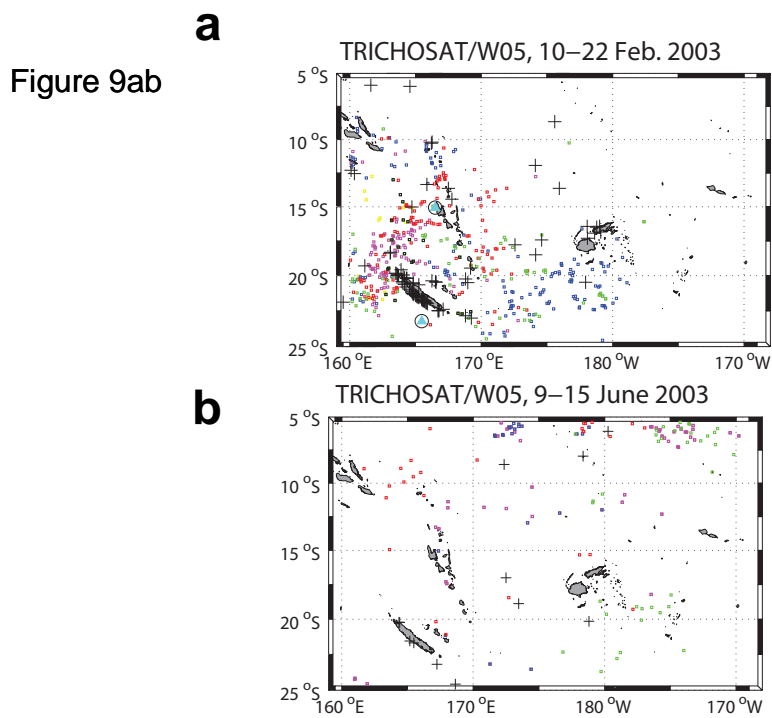


Figure 10

